Deep-Sea Research II 55 (2008) 1949–1963

Contents lists available at ScienceDirect

Deep-Sea Research II

journal homepage: www.elsevier.com/locate/dsr2

Bellingshausen and western Antarctic Peninsula region: Pigment biomass and sea-ice spatial/temporal distributions and interannual variabilty

Raymond C. Smith [a,b,*], Douglas G. Martinson [c,d], Sharon E. Stammerjohn [c,d], Richard A. Iannuzzi [c], Kirk Ireson [a]

[a] Institute for Computational Earth System Science, University of California, Santa Barbara, CA 93106, USA
[b] Department of Geography, University of California, Santa Barbara, CA 93106, USA
[c] Lamont-Doherty Earth Observatory of Columbia University, Palisades, NY 10964, USA
[d] Department of Earth and Environmental Sciences, Columbia University, New York, NY 10027, USA

ARTICLE INFO

Article history:
Accepted 21 April 2008
Available online 31 July 2008

Keywords:
Antarctic zone
Western Antarctic Peninsula
Pigment biomass
Sea ice
Southern Antarctic Circumpolar Current Front
Polar marine ecosystem

ABSTRACT

The Palmer Long-Term Ecological Research (LTER) program seeks to obtain a comprehensive understanding of various components of the Antarctic marine ecosystem—the assemblage of plants, microbes, animals, ocean, and sea-ice south of the Antarctic Polar Front. A central hypothesis of the Palmer LTER is that the seasonal and interannual variability of sea ice affects all levels of the Antarctic marine ecosystem, from the timing and magnitude of seasonal primary production to the breeding success and survival of apex predators. In the context of this high-latitude ecosystem we use satellite imagery to examine physical forcing and possible mechanisms influencing the distribution of phytoplankton biomass in the region to the west of the Antarctic Peninsula. We evaluate the spatial and temporal variability of pigment biomass (estimated as chlorophyll-*a* concentrations using SeaWiFS data) in response to the spatial and temporal variability of sea-ice extent (estimated from passive microwave satellite data). While the ocean-color data record is relatively short (7 years) and contains high interannual variability, there are persistent spatial patterns of phytoplankton biomass that indicate important regional-scale physical mechanisms including: the marginal ice zone and its impact on the mixed-layer depth, the timing of spring sea-ice retreat, the importance of the southern Antarctic Circumpolar front, and teleconnections with sub-polar regions. The SeaWIFS imagery presented here provides the most complete synoptic space/time views of phytoplankton biomass within this region to date. These observations suggest that the southern Antarctic Circumpolar front may have a more profound influence on the western Antarctic Peninsula ecosystem than previously thought.

1. Introduction

1.1. Background

Polar regions play a unique and important role in global climate and are thought to be the most sensitive regions on the planet to global change. Polar ecosystems are both characterized and dominated by the influence of sea ice. Locally, sea ice has an influence on air temperature and the exchange of heat, moisture and momentum between the atmosphere and the ocean. Regionally, sea ice influences cloud cover, water vapor and the surface albedo. On local to regional scales various feedback mechanisms operate to influence global climate via both dynamic and thermodynamic processes (Kellogg, 1983; Walsh, 1983; Rind et al., 1995, 2001; Church, 2001; Liu et al., 2003, 2004).

The Southern Ocean in particular has been recognized as one of the most important regions in the global marine carbon cycle, and its response to global warming is predicted to have a large impact on oceanic CO_2 uptake (Sarmiento and Le Quere, 1996; Sarmiento et al., 1998; Gille, 2002). The marine ecosystem of the Southern Ocean is considered to be globally significant, comprising one of the largest readily defined ecosystems on Earth (Harris and Stonehouse, 1991; Busalacchi, 2004). Evidence suggests that this ice-dominated ecosystem is balanced on the ice/water temperature threshold, and thus there is the potential for a strong non-linear response as the system "shifts" from mostly ice-covered waters to ice-free waters (Smith et al., 2003a).

The area west of the Antarctic Peninsula is an important component of the Antarctic marine ecosystem and is the focus of the Palmer Long-Term Ecological Research (PAL LTER) program (Smith et al., 1995; Ross et al., 1996; Ducklow et al., 2007). The

* Corresponding author at: Institute for Computational Earth System Science, University of California, Santa Barbara, CA 93106, USA.
E-mail address: ray@icess.ucsb.edu (R.C. Smith).

0967-0645/$ - see front matter © 2008 Elsevier Ltd. All rights reserved.
doi:10.1016/j.dsr2.2008.04.027

western Antarctic Peninsula (WAP) marine ecosystem is composed of a Coastal And Continental Shelf Zone (CCSZ) that is annually swept by sea ice and, hence, the marginal ice zone. Significantly, the WAP has experienced a statistically significant warming trend during the past half century (King, 1994: Stark, 1994; Smith et al., 1996a; King and Harangozo, 1998; Smith and Stammerjohn, 2001; Vaughan et al., 2003). As a consequence, this region is proving to be an exceptional area to study ecological response to climate variability (Ross et al., 1996; Smith et al., 1995, 1999b, 2003b; Domack et al., 2003) and to investigate how physical forcing influences the marine ecosystem and associated global biogeochemical processes.

Phytoplankton production plays a key role in the Southern Ocean marine ecosystem, and factors that regulate production include those that control cell growth (light, temperature and nutrients) and those that control cell accumulation rates and hence population growth (water-column stability, advection, grazing and sinking). The Southern Ocean is often referred to as a high-nutrient, low-chlorophyll (HNLC) region due to the persistence of relatively high levels of macro nutrients (nitrate and phosphate) but lower than expected associated phytoplankton biomass. In addition to light, biological productivity in the Southern Ocean may be limited by a general lack of iron (Martin and Fitzwater, 1988; Martin et al., 1990; Smetacek et al., 1997; Coale et al., 2004; Croot et al., 2004) or its availability in the euphotic zone (Rue and Bruland, 1995; Boye et al., 2001; Measures and Vink, 2001; and references therein). Several of the factors that regulate production are mediated by the annual advance and retreat of sea ice.

In the greater WAP (hereafter, extended WAP, or eWAP) region (Fig. 1), primary production closely follows the distribution of pigment biomass measured as chlorophyll-*a* (chl-*a*) concentration. Published values show a wide range of spatial and temporal variability (Moline and Prezelin, 1996; Smith et al., 1996b, 1998a, 2001; Dierssen et al., 2000; Garibotti et al., 2003, 2005). Garibotti et al. (2003) describe spatial distribution patterns of the phytoplankton community (composition, cell abundance and biomass concentration) in relation to local environmental conditions in the WAP area. They conclude that the large-scale variability in phytoplankton community structure is related to physical forcing (e.g., the spring sea-ice retreat) and to the seasonal succession of different algae groups. In investigating interannual variability Garibotti et al. (2005) found high stability in the composition and distributions of phytoplankton. The patterns that they observed (based on the vertical distribution of chl-*a*) are also in close agreement with those found by Martinson et al. (2008) based on the physical properties of the water column. Indeed, in agreement with Holm-Hansen and Mitchell (1991), Garibotti et al. (2005) show a close and non-linear relationship between phytoplankton biomass and the depth of the upper mixed layer, in agreement with the hypothesis that upper water-column stability, and its relation to the amount of solar radiation available to phytoplankton, is a dominant factor in regulating phytoplankton stocks.

The hydrography, circulation, heat and salt budgets have been described for the WAP area (Pollard et al., 1995; Hofmann et al., 1996; Hofmann and Klinck, 1998; Klinck, 1998; Smith, et al., 1999a; Beardsley et al., 2004; Dinniman and Klinck, 2004; Martinson et al., 2008). The Antarctic Circumpolar Current (ACC) flows northeasterly along the shelf break, and there is evidence of a southwestward-flowing coastal current on the inner part of the shelf (Moffit et al., 2008). The introduction of warm salty Circumpolar Deep Water (CDW) onto the WAP continental shelf is pervasive and brings macronutrients and dissolved inorganic carbon onto the shelf. The presence of this water mass near the bottom of the mixed layer is important for heat, salt, nutrient and carbon budgets in this region.

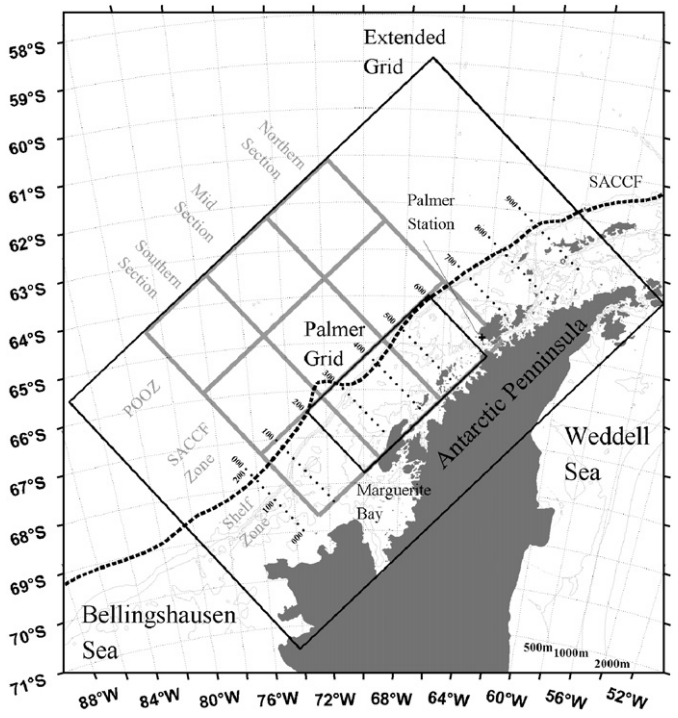

Fig. 1. Chart of the Western Antarctic Peninsula (WAP) region and the Palmer LTER (PAL) and extended Palmer LTER sampling grids. Dots represent ship sampling stations (perpendicular to the peninsula, the stations are 20 km apart, along the peninsula the sampling lines are 100 km apart) and demark the PAL grid. Palmer Station, and the fine-scale temporal sampling grid is located on the southern end of Anvers Island (64°46′S, 64°03′W). The 500 m isobath represents the continental shelf break (1000 and 2000 m isobaths also shown). The extended (satellite) Palmer LTER sampling grid, which encompasses the PAL grid, is shown by the larger box. The smaller box outlines the area within the 200–600 lines where most of the January ship-based observations have been located. The heavy dashed line gives the approximate location of the SACCF (Orsi et al., 1995; Martinson et al., 2008). Shaded boxes indicate sub-regions (NE–SW) and zones (on-to-offshore) discussed in the text.

The eWAP region is characterized by a strong climatic gradient between a cold dry continental regime to the south and a warmer moist maritime regime to the north. This gradient provides the potential for these regimes to shift in dominance from season-to-season and year-to-year, thus creating a highly variable environment that is sensitive to climate change (King, 1994; Smith, et al., 1999b, 2003a; Vaughan et al., 2001; King et al., 2003). Movement of this climatic gradient gives rise to significant variability in storminess, and there is some indication that low-pressure systems are larger and deeper in this area (Simmonds, 2003). Typically storminess is strongest during fall and spring. However, recent observations indicate an increase in storminess from early spring to late fall, thus impacting in particular the timing of sea-ice retreat and the subsequent advance, respectively (Stammerjohn et al., 2008a). In addition to warming, there is a trend toward increased precipitation (Turner et al., 1997, 2005). Also, the region shows clear co-variability with global climatic indices such as El Niño Southern Oscillation (ENSO) (e.g., Smith et al., 1996a; Harangozo, 2000; Carleton, 2003; Kwok and Comiso, 2002; Liu et al., 2002a, b; Yuan and Martinson, 2000, 2001; Yuan, 2004; Stammerjohn and Smith, 1997) and the Southern Annual Mode (SAM) (e.g., Hall and Visbeck, 2002; Lefebvre et al., 2004; Liu et al., 2004; Marshall et al., 2004).

Sea ice is a dominant and distinguishing characteristic of this marine ecosystem. The growth and ablation of sea ice affect the salinity, and hence density, gradients of the upper ocean. This, in turn, influences the vertical structure of phytoplankton distributions and abundance. Consequently, sea-ice dynamics can mediate the timing and areal extent of phytoplankton production.

Within the southern Bellingshausen Sea region (inclusive of the eWAP) observations of sea-ice variability during the satellite era show, in spite of high interannual variability, both a decrease in concentration and ice-season duration, whereas elsewhere in the Southern Ocean trends are generally weak except for the strong positive trends in the western Ross Sea (Jacobs and Comiso, 1997; Stammerjohn and Smith, 1997; Smith and Stammerjohn, 2001; Watkins and Simmonds, 2000; Zwally et al., 2002; Parkinson, 2002, 2004; Vaughan et al., 2003; Liu et al., 2004). It is within this highly variable physical environment that we consider the spatial and temporal variability of pigment biomass within the eWAP region on intraseasonal to interannual timescales.

1.2. Approach

In the following, we utilize satellite data from various sources (discussed below) over a 7-year period (October 1997 to April 2004) to examine pigment biomass, sea ice, wind and surface solar irradiance on seasonal to interannual time scales and over an area west of the Antarctic Peninsula covering nearly a million square kilometers (i.e., the eWAP, Fig. 1). Previous satellite-based synoptic views of pigment biomass (Sullivan et al., 1993; Smith et al., 1998a, 2001) made use of the earlier, although comparatively limited, Coastal Zone Color Scanner (CZCS) data. The SeaWIFS imagery presented here provides the most complete synoptic space/time views of phytoplankton biomass within this region to date. We evaluate observed patterns of pigment biomass in the eWAP with a focus on the potential influence of sea ice on these patterns. We evaluate the spatial-temporal patterns of phytoplankton distributions within the context of possible physical controls influencing those patterns including: (1) the influence of the marginal sea-ice zone (MIZ) on mixed-layer depth (MLD) and the timing of springtime sea-ice retreat; (2) the influence of the Southern Antarctic Circumpolar Current Front (SACCF) on phytoplankton productivity; (3) the influence of climate variability on high-latitude atmospheric circulation changes; and (4) the variability in photosynthetic available radiation (PAR).

1.2.1. Mixed-layer depth

Phytoplankton blooms require relatively shallow MLDs like those found in the marginal ice zone during spring, which are created by the melt of retreating sea ice. This hypothesis (or slight variations thereof) has been suggested by numerous authors (Smith and Nelson, 1985, 1986; Nelson et al., 1987; Holm-Hansen and Mitchell, 1991; Sullivan et al., 1993; Smith et al., 1998a; Garibotti et al., 2003, 2005) and is described as follows. Stability within the MIZ is enhanced by the melt water from sea ice and by solar warming of the now ice-free surface waters. Phytoplankton growth and accumulation, perhaps seeded by algal cells released from sea ice, take place in this stable and well-lighted upper water column. Spatially, the ice-edge bloom is expected to be restricted to within a few hundred kilometers following the retreating ice edge. Temporally, the bloom involves active growth followed by decay and/or dissipation with reported time scales of days to a few months.

1.2.2. Southern Antarctic Circumpolar Current Front

Hydrographic fronts are important in determining the location and seasonal progression of enhanced pigment biomass. In particular, high pigment biomass may be associated with the southern limit of the ACC that separates the Antarctic Zone to the north from the Continental Zone to the south (hereafter referred to as the SACCF as defined by Orsi et al. by the 0.35 geopotential height contour and southern limit of upper CDW) (Orsi et al., 1995; Tynan, 1998). In the WAP region the southern limit of the ACC regularly lies near the continental shelf break as indicated in Fig. 1 (Orsi et al., 1995; Martinson et al., 2008). This frontal region was also investigated in detail by the United Kingdom "Sterna" study in the Bellingshausen Sea as part of the Southern Ocean JGOFS work (Turner and Owens, 1995; Pollard et al., 1995). These studies took place just to the west of our eWAP area around 68°S, 85°W.

1.2.3. Climate variability

Atmospheric circulation anomalies associated with various climate modes play an important role in modulating both sea-ice and phytoplankton productivity. For example, throughout the South Pacific and western South Atlantic sectors of the Southern Ocean, studies have shown strong co-variability between sea ice and ENSO (Simmonds and Jacka, 1995; Harangozo, 2000; Yuan and Martinson, 2000; Venegas et al., 2001; Kwok and Comiso, 2002). There also is increasing evidence that the variability in the Southern Annular Mode (SAM) is a strong influence on sea-ice variability as well (Hall and Visbeck, 2002; Lefebvre et al., 2004; Liu et al., 2002a, 2004; Stammerjohn et al., 2008a), particularly in the 1990s, which saw a relatively high occurrence of the strong positive phase of SAM (Thompson and Wallace, 2000; Thompson and Solomon, 2002; Marshal, 2003). In addition, there is the potential for the high-latitude ENSO response to be modulated by SAM (or vice-versa) in the eastern Pacific sector of the Southern Ocean given this area's sensitivity to both climate modes (Simmonds and King, 2004), and several recent studies show this to be the case (Silvestri and Vera, 2003; Liu et al., 2002a, 2004; Carvalho et al., 2005; Fogt and Bromwich, 2006; L'Heureux and Thompson, 2006; Stammerjohn et al., 2008a). The documented long-term warming trend coupled with quasi-periodic variability driven by the high-latitude response to climate variability likely plays a role in modulating the observations discussed here. Consequently, we expect the observations of pigment biomass to be influenced by such global-scale climate variability.

1.2.4. Photosynthetic available radiation

Surface solar irradiance is essential for phytoplankton productivity, and the seasonal progression of PAR gives rise to the large-scale seasonal variability observed in phytoplankton biomass at these high latitudes. Indeed, a separate analysis (to be published elsewhere), shows that over 50% of the variability in pigment biomass is explained by variability in incident PAR. However, the space/time variability of solar radiation, due to cloud cover and/or variable stratospheric ozone, is on a shorter temporal scale than considered in this analysis, which makes use of monthly pigment biomass averages.

1.2.5. Grid, zones and sections

To assist in identifying possible controls on pigment biomass variability as highlighted above, we separated (averaged) the data into various zones extending on-to-offshore and sections alongshore. The on-to-offshore zones conformed to distinct biogeochemical provinces, while alongshore sectors serve to highlight possible north-to-south differences responding to long-term changes driven by global warming, i.e., changing trophic structure driven by climate migration (Smith et al., 2003a, c).

The Antarctic marine ecosystem has long been viewed in terms of zonal biogeographical (Hart, 1942) and, more recently hydrographic and biogeochemical, subdivisions (Longhurst, 1998). Tréguer and Jacques (1992) identified four on-to-offshore subdivisions within the Southern Ocean which are delineated by major frontal systems, and which are based on mechanisms controlling nutrient dynamics and hence phytoplankton

production: (1) a highly productive CCSZ, (2) a relatively productive Seasonal Ice Zone (SIZ, that area annually covered by sea ice), (3) a less productive Permanently Open Ocean Zone (POOZ), and (4) a Polar Front Zone (PFZ). The PFZ occurs northwest of our extended grid and will not be highlighted here. The first three zones occur within our extended grid, and we have introduced a fourth region, represented by the SACCF zone (as described above) that lies between the CCSZ and POOZ zones and within the SIZ zone.

1.2.6. Objectives

Our objectives are as follows: (1) utilize satellite data to evaluate spatial patterns and seasonal to interannual variability of pigment biomass over an extended region west of the Antarctic Peninsula; and (2) identify possible mechanisms that could give rise to the observed patterns of pigment biomass variability. In particular, we seek to identify potential mechanisms responsible for the timing of the seasonal patterns. The evaluation of pigment biomass variability over the extended grid also provides a larger context, as well as a seasonal context, for the LTER annual January cruises. This information will be used to optimize future multi-platform sampling strategies (e.g., continued satellite coverage and ship-based sampling, as well as the deployment of *in situ* gliders and moorings).

2. Data and methods

2.1. Sampling strategy and analysis domain

The Palmer LTER (PAL) long-term observations are structured by a sampling grid (Waters and Smith, 1992) that lies along the west coast of the Antarctic Peninsula (Fig. 1). This fixed grid provides station locations that can be visited repeatedly over time scales of many years, simplifies seasonal and interannual comparisons and facilitates analysis and modeling of multi-disciplinary data sets. The Palmer LTER grid is 1000 km roughly parallel to the peninsula and 200 km on-to-offshore. Transect (grid) lines are perpendicular to the peninsula, spaced every 100 km, and numbered 000.sss to 900.sss, where the sss is the station line (e.g., station 600.040 lies 40 km offshore on the grid line 600 km along the peninsula). PAL surface data are obtained using three basic modes of sampling: (1) weekly time series data collected roughly between November and March within the two-mile boating limit near Palmer Station; (2) regional data collected during six-week research cruises every January through early February that covers much of the PAL grid; and (3) process oriented cruises every few years during other seasons. Typically, our annual January cruises encompass the 200–600 transect lines and cardinal stations are spaced every 20 km apart from near shore (xxx.000) to 200 km offshore (xxx.200 (small box in Fig. 1)). The annual sampling is timed to match a critical period in the breeding chronology of the Adelie penguin (*Pygoscelis adeliae*). Cruise data include physical, optical, chemical and biological observations within this 200×400 km region that also includes LTER-censused penguin colonies. Surface observations discussed herein were obtained within the PAL grid.

Satellite data complement surface observations and extend our ship-based and near-shore observations both seasonally and regionally (Smith et al., 1998a, 2001). In the following we use the eWAP region (Fig. 1), or "extended grid", that encompasses the PAL grid but which is roughly 12 times its area (large box in Fig. 1). The larger domain of the extended grid includes mechanisms that also are operating within the smaller PAL grid or heavily influence the variability observed there.

2.2. SeaWiFS data and derived parameters

Global and regional maps of the upper-ocean chlorophyll concentration estimated from ocean-color satellite data have been used for over two decades (Hovis et al., 1980; Gordon and Morel, 1983; Gordon et al., 1983; Siegel et al., 2004; Behrenfeld et al., 2005), various products are being generated routinely from SeaWiFS data by the Goddard Earth Sciences Data and Information Services Center Distributed Active Archive Center (DAAC, http://oceancolor.gsfc.nasa.gov), and recently two Deep-Sea Research Topical Studies volumes have been devoted to SeaWiFS observations (Siegel et al., 2004). For the work reported here, we use Global Area Coverage (GAC) standard mapped data that utilize the OC4V4 algorithm (O'Reilly et al., 1998, 2000) for the time period from September 1997 through April 2004, (i.e., seven spring-to-autumn seasons). Monthly means were computed using the maximum likelihood estimator mean. The resolution of each pixel in the image is approximately 0.088° latitude by 0.088° longitude, which translates roughly to 9.77 and 4.2 km per pixel in the north–south and east–west directions, respectively, for the latitudes considered here. Land, clouds and sea ice have been masked from the images prior to use.

Bio-optical properties of Antarctic waters are significantly different than those at temperate latitudes. As a consequence, general ocean-color processing algorithms (e.g., for CZCS, SeaWiFS, MODIS) result in an underestimate of chlorophyll in Antarctic waters by roughly a factor of two (Mitchell and Holm-Hansen, 1991; Sullivan et al., 1993; Smith et al., 1998a; Moore et al., 1999; Moore and Abbott, 2000; Dierssen and Smith, 2000; Dierssen et al., 2000; Korb et al., 2004). We previously used bio-optical observations in the LTER region to develop an ocean-color algorithm (SO-algorithm) for Antarctic waters (Dierssen and Smith, 2000) and to develop optimized models for remotely estimating primary production (Dierssen et al., 2000). Further, during the lifetime of the SeaWiFS ocean-color satellite sensor (Sept 1997 to Jan 2005) we made *in situ* bio-optical observations including: (1) profiles of pigment concentrations using both fluorometric and high-performance liquid chromatography (HPLC) techniques, and (2) profiles of downwelling spectral irradiance (E_d) and upwelling spectral radiance (L_u) using a free-fall Profiling Reflectance Radiometer (PRR). We use these bio-optical observations to augment our earlier algorithm, focusing on contemporaneous SeaWiFS ocean-color satellite data to create an LTER SO-algorithm.

Bio-optical properties (e.g., absorption, scattering, attenuation, reflectance, etc.) are linked to regional distributions of dissolved (e.g., DOM, DIM) and suspended (e.g., phytoplankton and their respective pigments) material, which in turn characterize an in-water algorithm. Thus, the unique characteristics of the LTER SO-algorithm result from the unique bio-optical properties of these high-latitude waters. A validation of the SO-algorithm using SeaWiFS data shows that satellite-derived chl-*a* can be used to accurately estimate chl-*a* in these waters (Dierssen and Smith, 2000). For the following analysis, all satellite-derived chl-*a* are adjusted using the SO-algorithm and increase chl-*a* by a factor of two. However, the emphasis of this work is on the spatial patterns of chlorophyll and their variability, which are mostly unaffected by this adjustment. The absolute chlorophyll values and our SO-algorithm will be addressed in detail elsewhere.

2.3. Passive microwave sea-ice data and derived variables

Passive microwave remote sensing of the Southern Ocean provides one of the most complete space/time records of the annual advance and retreat of sea ice, because neither clouds nor

winter polar darkness limit microwaves. Consequently, these data are exceedingly valuable in both describing and understanding the highly variable physical environment affecting the marine ecology of polar regions. The passive microwave data used in this study are from NASA's Scanning Multichannel Microwave Radiometer (SMMR) and the Defense Meteorological Satellite Program's (DMSP) Special Sensor Microwave/Imager (SSM/I) from which sea-ice concentrations were determined using the GSFC Bootstrap passive microwave algorithm (Comiso, 1995; Comiso, 2003). The SMMR and SSM/I monthly sea-ice concentration data were intercalibrated and merged into one time series to minimize differences between the SMMR and SSM/I sensors (Comiso et al., 1997). The EOS DAAC at the National Snow and Ice Data Center (University of Colorado in Boulder, Colorado, http://nsidc.org) provided the SMMR–SSM/I time series data. Methods and details regarding these data are given elsewhere (Stammerjohn, 1993; Stammerjohn and Smith, 1996; Smith et al., 1998b; Smith and Stammerjohn, 2001; Stammerjohn et al., 2003). The satellite-derived estimates of sea-ice extent (i.e., the area enclosed by the ice edge) are provided on a daily basis with a pixel resolution of 25 km^2. Our previous studies have demonstrated that both the timing and magnitude of sea-ice coverage are variable from year to year and that sea-ice dynamics can mediate the timing and area extent of production at the base of the food web.

2.4. Analytical methods

For each of the months for which there is sufficient light and open water for satellite observation of pigment biomass (October through April) and for each of the 50×100 km grid cells in the extended grid we calculate the monthly average data. From the seven years of monthly average data, we computed a monthly climatology and the anomalies about that climatology. These results are presented as maps (climatology in Fig. 2 and anomalies in S.M. 2).

We use empirical orthogonal function (EOF) decomposition of the individual monthly time series (e.g., October 1997–2003, November 1997–2003, December 1997–2003, January 1998–2004, etc.) to examine the dominant monthly spatial patterns. Estimation techniques are used to calculate the EOFs where there are data gaps. The principle components (PCs) are calculated from the EOFs and describe the temporal evolution of the EOF spatial patterns. In this study we show only the first mode, i.e., the mode that explains the majority of the (decomposed) variance. Full details on the methods used in extracting and selecting the dominant (mode 1) EOF and PC are described by Martinson and Iannuzzi (2003) and Martinson et al. (2008). For completeness, the first four modes that capture more than 80% of the variance are given in S.M. 3.

Supplementary materials may be accessed at: 〈http://pal.lternet.edu/docs/doi/pallter0304〉.

3. Results

3.1. Climatology and seasonal cycles

The monthly (September through April) climatology images of SeaWiFS-derived chl-*a* are shown in Fig. 2. The climatology images were computed from the 7 years of monthly composites, 56 images total, which comprise the most comprehensive synoptic data for this area to date and can be found in the Supplementary Material (S.M. 1). Also provided as Supplementary Material are the anomaly maps for each month (S.M. 2a), as well as the number of observations included in computing the climatologies and monthly composites, respectively (S.M. 2b). Cloud cover, low solar elevation and sea ice limit the SeaWiFS data in this region. Sea ice, in particular, limits coverage early and late in the season, which is why there are no values in the southern part of the grid (lower right) for the months of September, October, November and April.

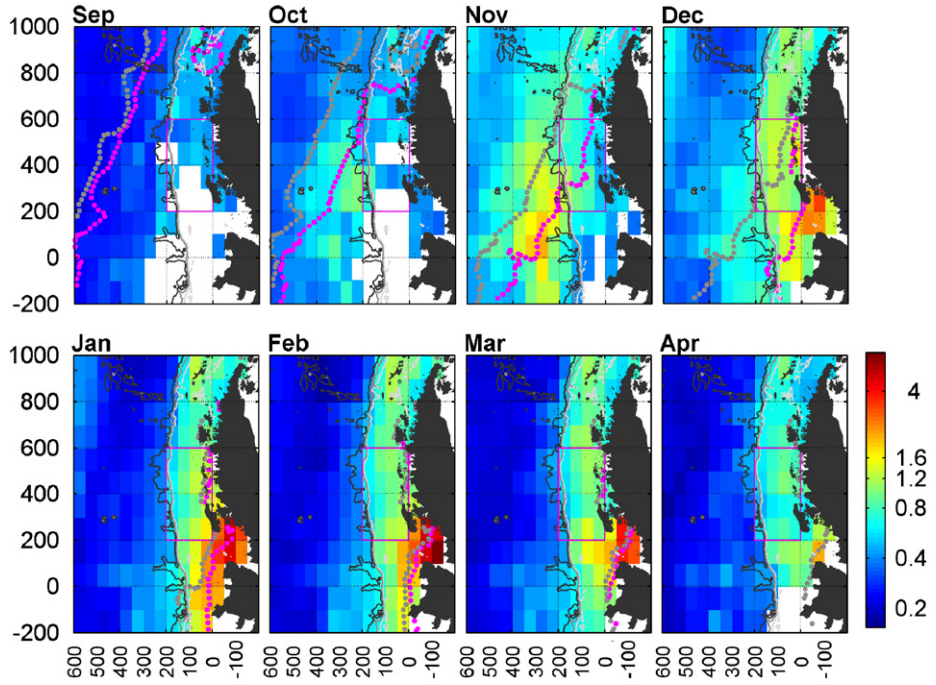

Fig. 2. Monthly chl-*a* climatologies (based on LTER SO algorithm and seven years of SeaWiFS data) for the extended grid area off the west coast of the Antarctic Peninsula (mg chl-*a* m^{-3}). Bathymetry lines are shown for 500, 1000 and 2000 m depth contours (grey to black). Magenta box outlines the PAL grid (between the 200 and 600 lines). Monthly anomalies, corresponding to the monthly climagologies, are shown in S.M. 2a. Grey dotted line represents the mean (seven year) sea-ice extent at the beginning of the month and the purple dotted line the mean extent at the end of the month. White areas indicate limited data due to sea-ice coverage.

The monthly climatology images display most notably an off-to-onshore seasonal pattern and provide a regional-scale context for pigment biomass (a rough proxy for phytoplankton production) in the area. They also provide a perspective as to how, on average, sea ice influences pigment biomass in the WAP area. During September both the extended and PAL grids are mostly covered by sea ice (dotted grey and purple lines indicate the mean position of the ice edge at the beginning and end of each month, respectively). When open water is observed, the September climatology shows very low chl-*a* values seaward of the sea ice, with values less than 0.2 mg m^{-3}. Late winter to early spring (August, September and October) also is characterized by relatively strong winds (as seen in the monthly composites, S.M. 1, featuring mean monthly wind speeds on the order of 4–6 m s^{-1}) and deep mixing, thus unfavorable conditions for phytoplankton growth. We recognize that the NCEP Reanalysis wind data, especially when considering monthly averages, poorly represent strong wind events. However, we include these data on the composite images as a rough indicator of seasonal variability in wind forcing. The monthly anomalies for these wind data (not shown) indicate there is considerable variability in wind speed and direction from year-to-year.

The months of October and November show the beginnings of a spring phytoplankton bloom within the extended grid. Sea ice typically retreats a few hundred kilometers in each of the months of October and November, with higher pigment biomass generally following the sea-ice retreat (discussed in detail below). The climatology for October shows an early spring bloom (~1 mg m^{-3}) forming roughly 200–400 km offshore and centered between the 200 and 400 grid lines (perpendicular to the peninsula). Seaward of the ice edge the chl-*a* concentration is typically less than 0.2 mg m^{-3}. By November, this moderate bloom becomes more developed within roughly the same offshore area as seen in October while spreading southwest and northeast along the shelf break. It is important to note that the beginning and ending sea-ice extent lines are a mean position for the seven-year climatology, but in the anomaly figures (S.M. 2) the actual monthly beginning and ending sea ice positions are shown. Chlorophyll concentrations over the shelf typically remain relatively low during October/November, often because of sea-ice cover. By the end of December, most of the sea ice has retreated in the eWAP, except for areas south of 68°S (roughly, south of our 200 line) and within Marguerite Bay. Bloom levels of pigment biomass (>1 mg m^{-3}) are now concentrated primarily over the shelf within 200 km of the peninsula. Chlorophyll concentrations seaward of the shelf break are now lower than was observed earlier in the season. Sea ice is typically gone from the shelf by January and February, bloom levels of pigment biomass are now mostly along the coast and very low levels (<0.2 mg m^{-3}) are found seaward of the shelf break. Relatively high values of pigment biomass (mean values ~2–5 mg m^{-3}) are found in Marguerite Bay and close to the coast in the more southerly part of the grids. These coastal-dominated patterns of pigment biomass remain through March and April, but with decreasing concentrations as fall transitions into winter. Seaward of the shelf break, pigment biomass is consistently low (<0.2 mg m^{-3}) from January through April.

3.2. Interannual variability

As described in Section 2.4, we used classical Principle Component Analysis (PCA) to compute the EOFs and PCs from the seven years of monthly data (S.M. 1) following Martinson (Martinson and Iannuzzi, 2003). The PCA distills those many images into dominant features in space (the EOFs) and time (the PCs), making this a very useful approach to assess interannual variability. The gravest mode describes between one-third to more than one-half of the variability in each month, and Fig. 3 shows the first mode of the EOFs and PCs for each month. Grid cells with less than five years of data are left blank. While the EOFs capture the dominant spatial patterns that are coherent from year-to-year, the PCs show how the amplitude of that spatial pattern varies over 1997–2004. The off-to-onshore seasonal progression of high pigment biomass that was described for the climatology images in Fig. 2 are captured by the EOFs. Here we focus on the interannual variability as given by the PC.

Over the 1997 to 2004 time period, there were several years when pigment biomass was high from November to March: 1999–2000, 2000–2001 and 2001–2002. Conversely, there were two years when it was low: 1997–1998 and 2002–2003. The high biomass years co-occur with La Niña events, whereas the low biomass years co-occur with El Nino events, a correspondence

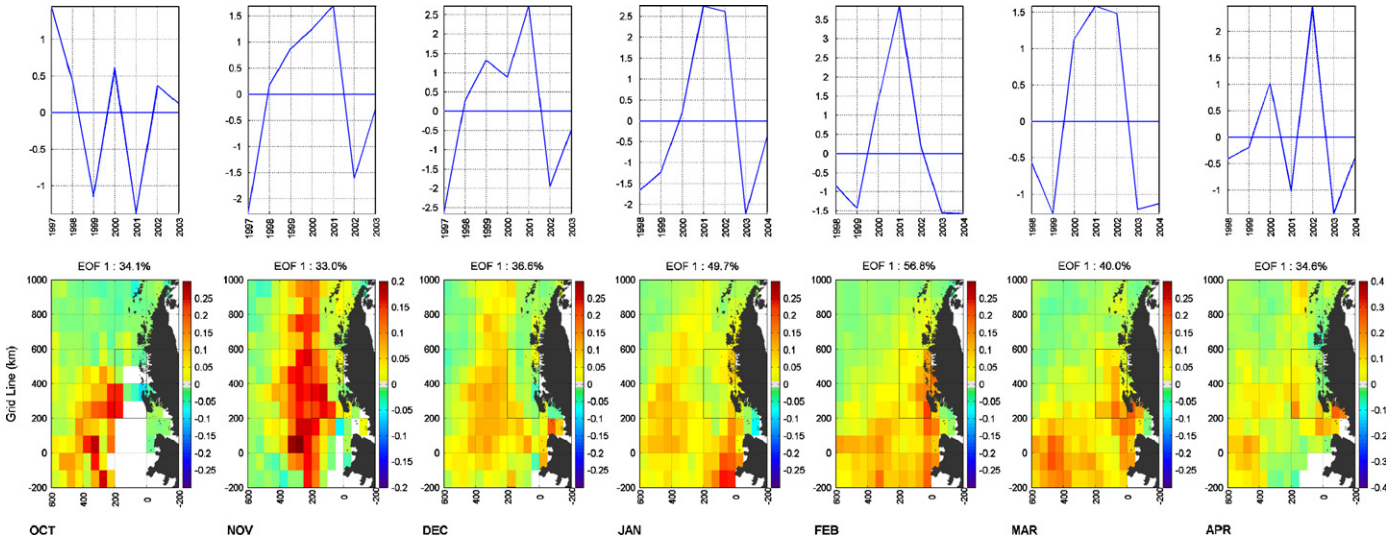

Fig. 3. Principle components (PCs) and spatial patterns (EOFs) from the decomposition of monthly chl-*a* anomalies showing the first mode. Percents show the amount of total variance described by the first mode. Principle components and spatial patterns for the first four modes, which capture over 80% of the variance, from the EOF decomposition of chl-*a* for each month are provided in S.M. 3. Note, that because austral summer falls across the year boundary, the year scale for October through December 1997 corresponds to the same season as the months January through April 1998, etc.

that will be examined and discussed in more detail in the next section. There also were two transitional years. In 1998–1999, biomass went from near-average values in October–December to anomalously low values in the subsequent January–March period, whereas in year 2003–2004, biomass went from slightly low values in November–January to anomalously low values in February–March. In general, the interannual variability in October and in April does not appear to follow the year-to-year seasonal variability described for the November-to-March time period. This may be due to stronger and more variable winds in early spring (October) and late autumn (April) and/or the variability associated with the ending and beginning of winter sea-ice cover.

3.3. Cross-shelf and along-shelf variability

We sub-divided the extended grid into on-to-offshore zones (as described in Section 1.2): the 'shelf' zone, 0–200 km from the Peninsula; SACCF zone, seaward of the shelf break and 200–400 km from the Peninsula; and the POOZ, 400–600 km from the Peninsula. We also evaluated the chl-*a* anomalies for three separate north-to-south (strictly north east to south west) sectors of the extended grid: where 'northern' encompasses grid lines 450–650 and is inclusive of the Palmer Station area; 'mid' refers to grid lines 250–450; and 'southern' to grid lines 050–250, which is inclusive of Marguerite Bay. Each of these areas (boxes outlined by shaded lines in Fig. 1) are 200 km × 200 km averages which are representative of their respective NE–SW sectors and on-to-offshore zones.

Fig. 4 displays seasonal chl-*a* time series for the above discussed NE-to-SW sectors, which have been averaged across onshore (0–200 km), mid (200–400 km) and offshore (400–600 km) zones. In addition, the 7-year climatology for each region and zone is displayed in the left hand graphs. Offshore waters (blue curves in Fig. 4) are uniformly low (typically $<0.5\ \mathrm{mg\,m^{-3}}$) and display a seasonal cycle that varies by roughly a factor of two (from 0.2 to 0.4 $\mathrm{mg\,m^{-3}}$), with higher values in the spring and lower values in the summer and fall. These waters are the least influenced by seasonal sea ice, and approximate geographically the POOZ (Tréguer and Jacques, 1992) as discussed in more detail below. Waters 200–400 km from the Peninsula, which are seaward of the shelf break, often display the highest spring phytoplankton blooms (green curves in Fig. 4). These are waters seasonally swept by sea ice and are influenced by the SACCF. However, these blooms decline rapidly, and only rarely are they followed by elevated values during the summer/fall period. In contrast, the areas over the shelf (0–200 km) generally peak later in the season (December to January) and often show a secondary summer/fall bloom (red curves in Fig. 4). These shelf waters also display greater variability in the seasonal timing of peak values, but show elevated chlorophyll over longer periods, thus giving rise to higher integrated seasonal values.

There is now considerable evidence that the Antarctic Peninsula region offers a natural laboratory to investigate how climate variability influences ecosystem response (Smith, et al., 1999b; Domack et al., 2003 and references therein). Various paradigms have been proposed for the way ecosystems may respond to climate variability (McCarthy et al., 2001). One, the modification paradigm (Kennedy, 2002), assumes that as climate

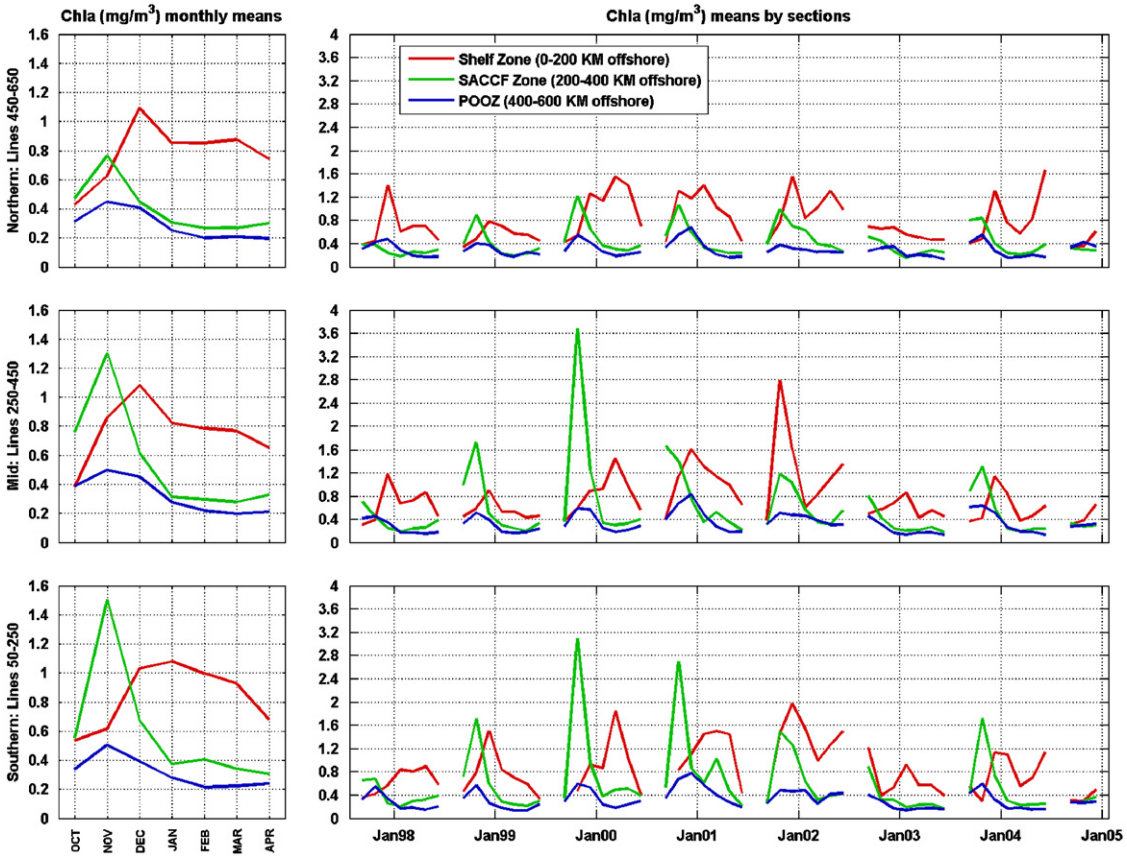

Fig. 4. Time series plots of (right side) chl-*a* concentrations ($\mathrm{mg\,m^{-3}}$) presented for southern (50–250 lines), mid-grid (250–450 lines) and northern (450–650 lines) sectors and for shelf (0–200 km, CCSZ, red curves), SACCF (200–400 km, green curves) and POOZ (400–600 km, blue curves) zones within the Palmer LTER extended grid. The same sectors and zones (left side) but presenting mean curves averaged over seven year time period.

and other environmental factors change, with a consequent shifting of the coevolved synchrony of the food web, there will be a change in the abundance, distribution and dominance of key species. Hypotheses linking sea ice and phytoplankton are suggestive of a north-to-south shift in maximum phytoplankton production in concert with the observed shorter sea-ice season in the WAP. Our observations span too short a time frame to establish trends, and we present north-to-south satellite observations as baseline data for longer-term studies.

3.4. Climate variability

In Fig. 5, chl-*a* anomalies for the extended grid are plotted for the seven seasons and seven years of SeaWiFS data. Also plotted in Fig. 5 are the anomalies for the Niño 3.4 index, normalized sea-surface temperature anomalies averaged over the eastern equatorial Pacific for 5°N–5°S, 170–120°W (Cane et al., 1986) and SAM index (Marshal, 2003). A positive Niño 3.4 index indicates El Niño conditions in the eastern tropical Pacific, while a negative index indicates La Niña conditions. The SAM index has been standardized and the Niño 3.4 axis inverted for ease of comparison.

Fig. 5 shows that our study period began during a very strong El Niño (1997–1998) and ended during a relatively strong El Niño (2002–2003) that bracketed three consecutive La Niña events (1998–1999, 1999–2000 and 2000–2001). As a consequence, this relatively short seven-year period experienced the extremes of an ENSO cycle. Chl-*a* and Niño 3.4 are anti-correlated ($r = -0.42$) so that roughly 18% of the observed interannual variability can be explained by linkage to this global source of climate variability.

Previous studies have documented strong co-variability between sea-ice extent in the WAP region and the ENSO (Smith et al., 1996a; Harangozo, 2006; Stammerjohn et al., 2008a). Those findings indicate that El Niño events are associated with cold southerly winds and positive sea-ice anomalies, while La Nina events are associated with warm northerly winds and negative sea-ice anomalies. More recent studies indicate that the high-latitude atmospheric circulation response to ENSO variability is strongest during the Austral spring-to-autumn period (Fogt and Bromwich, 2006; Stammerjohn et al., 2008a), with greatest impact in the WAP region during the spring sea-ice retreat and subsequent autumn advance.

In addition, the high-latitude atmospheric ENSO response appeared to have intensified beginning in the early 1990s as compared to the 1980s, with the intensification being more pronounced during La Niña events. Concurrently over this period SAM has become more positive, and the high-latitude atmospheric response to a positive SAM event is similar to the La Niña response in the WAP region (i.e., intensification of warm northerly winds and negative sea-ice anomalies, Stammerjohn et al., 2008a). Indeed, the two La Niña events in 1998–1999 and 1999–2000 depicted in Fig. 5 were also coincident with two strong positive SAM events during the spring-to-autumn period. In addition, there was a strong positive SAM event in 2001–2002, which may help to explain the continued high chl-*a* biomass observed during the spring–summer of 2001–2002 (despite the near neutral ENSO conditions). Whether more positive SAM events will continue to occur, and whether positive SAM events will continue to co-occur with La Niña events, remains to be seen, but these associations have been documented for the period of observations shown here, and as shown in Fig. 5, the ice–atmosphere response appeared to have a significant impact on pigment biomass. Potential mechanisms of the high-latitude atmosphere–ice response to ENSO and SAM variability and how that response might affect pigment biomass will be discussed in Section 4.

We note that in the 1980s and early 1990s, various climate variables in the Southern Ocean (sea ice, sea-level pressure, wind stress) displayed a seven- to 8-year oscillation known as the Antarctic Circumpolar Wave (ACW) that was linked to the high-latitude response to ENSO variability (White and Peterson, 1996). However, since the early 1990s the seven- to eight-year oscillation is no longer apparent, though the high-latitude response to ENSO variability remains strong. Thus, the biomass variability shown in Fig. 5 for 1997–2004 is not believed to be related to the ACW, but does appear to be related to ENSO variability with the potential additional influence or modulation by SAM variability as described above.

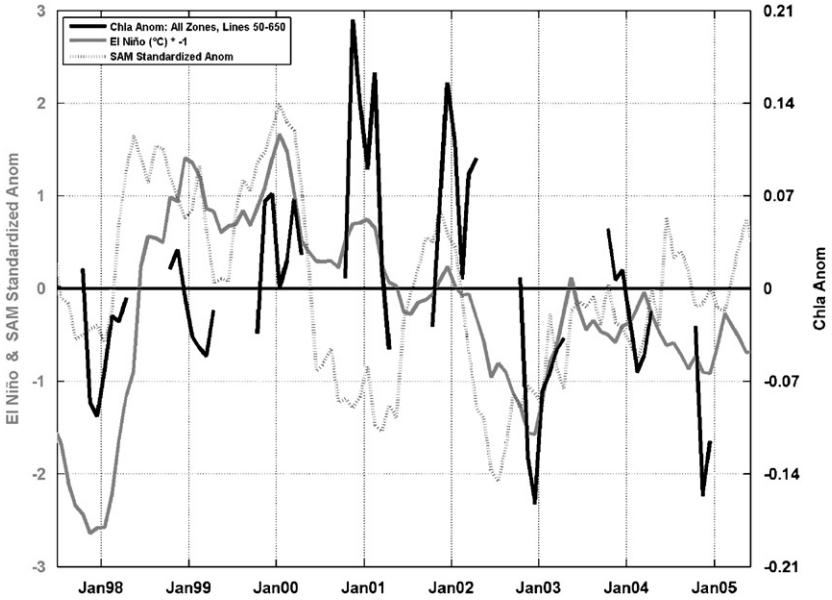

Fig. 5. Anomalies of chl-*a* (black), Niño 3.4 index (grey) and standardized SAM anomaly (dashed, computed as the monthly value minus the mean for that month for the years shown, divided by the standard deviation for the years shown) versus time (October 97 through April 2004). Chl-*a* anomaly was computed for all sectors, i.e., grid lines (50–650) and zones (000–600 km). Chl-*a* anomalies and Niño 3.4 are anti-correlated ($r = -0.42$) so the Niño 3.4 anomaly is plotted with a change of sign on the vertical axis for ease of comparison. SAM indices were smoothed with a seven point running mean.

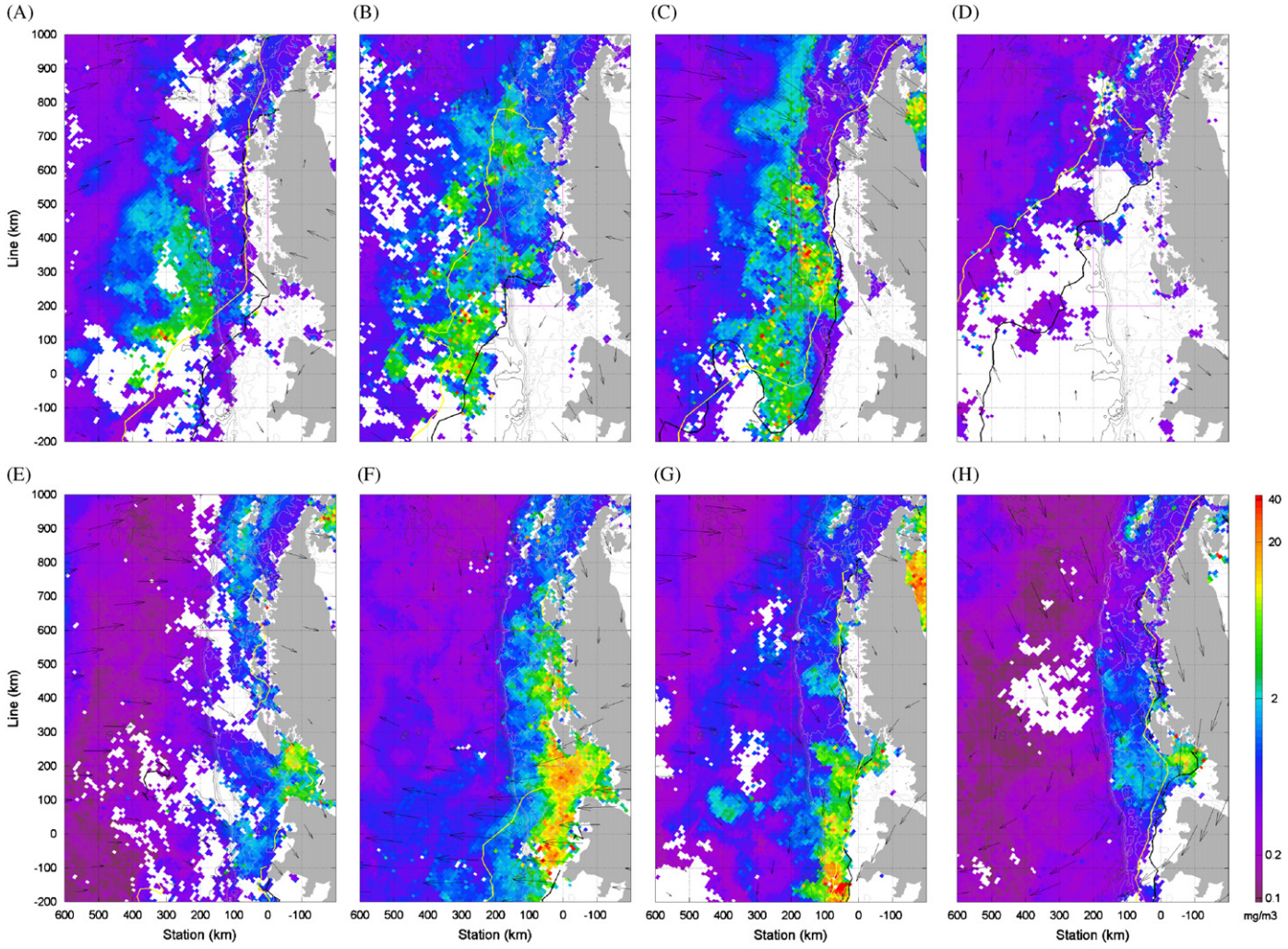

Fig. 6. Representative SeaWiFS GAC monthly images for the extended grid for (A) November 1998, (B) November 2000, (C) November 2001, (D) November 2002, (E) January 1999, (F) January 2001, (G) January 2002 and (H) January 2003. Location of sea ice at the beginning of the month (from SSM/I data) indicated by the yellow line and the location at the end of the month is shown by the black line. White/grey lines show 500, 1000 and 2000 m bathymetric contours. Arrows indicate monthly averaged (10 m) wind data from the NOAA National Center for Environmental Prediction/National Center for Atmospheric Research (NCEP-NCAR) Climate Data Assimilation System 1 (CDAS-1) generated by the NCEP-NCAR Reanalysis Project (Kalnay et al., 1996). These are representative images from our period of analysis, October 1997 through April 2004. All the monthly composites used in these analyses may be found in the Supplementary Material (S.M. 1).

3.5. *Evaluation of spatial patterns*

Fig. 6 combines three independent sets of satellite data for two representative months (November and January) and four representative years (1998–1999, 2000–2001, 2001–2002 and 2002–2003). The underlying image is the chl-*a* concentration [mg m^{-3}] estimated from monthly averaged SeaWiFS data. The yellow line indicates the sea-ice edge at the beginning of the month and the black line the ice edge at the end of the month as determined using passive microwave data. We use the area between the beginning and ending ice edge for each month as a satellite-determined estimate of the marginal ice zone (MIZ), the area potentially stabilized by sea-ice melt water. Arrows show the monthly averaged wind data. In total, we present 56 such composite images (S.M. 1), spanning the period from September 1997 through April 2004 (8 months in each of 7 years).

There are limited complementary surface observations in the Southern Ocean. Though the patterns of phytoplankton distributions in the SeaWiFS images suggest possible mechanisms, to fully test these mechanisms additional complementary surface observations are required. Nonetheless the synoptic space/time satellite data are suggestive of processes and/or hypotheses that wait future testing when such data become available. In the following, we discuss a few selected images from the months of November and January that are illustrative of potential mechanisms influencing the observed patterns.

3.5.1. *Marginal sea-ice zone*

It is known that phytoplankton blooms require relatively shallow MLDs like those found in the MIZ during spring, which are created by the melt of retreating sea ice (see Section 1.2 for a more complete description of this proposed mechanism). If this process were influencing the spatial pattern of pigment biomass, then the observed blooms would follow the spring retreat of the ice edge, roughly within the MIZ (between the yellow and black lines) as defined above.

Fig. 6A and B (November 1998 and 2000) provide examples of a pattern where the area of sea-ice retreat (the satellite estimated MIZ) show low and elevated chlorophyll values, respectively. Surface observations are necessary to fully characterize the area where sea-ice melting has stabilized the water column, and our satellite estimate of the MIZ must be viewed as only a first-order

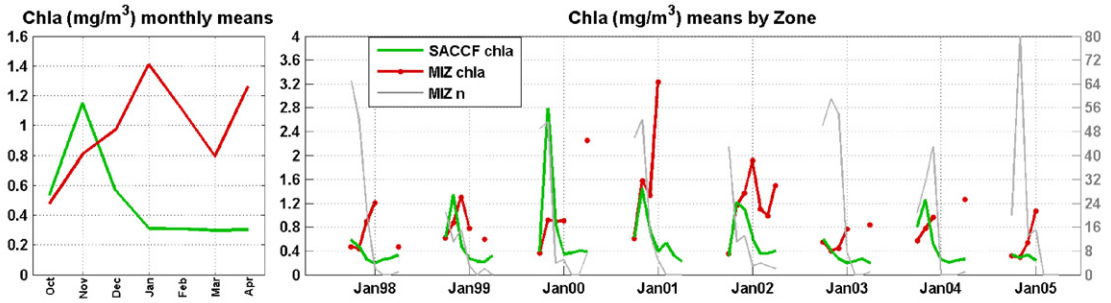

Fig. 7. Time series plots of (right side) chl-*a* concentrations (mg m^{-3}) presented for the SACCF (200–400 km, green curves as in Fig. 4) and the MIZ as estimated from satellite sea-ice data (red curves). The area of MIZ is taken as that area between the beginning and ending ice-edge positions for each month. Average chl-*a* concentration is the average SeaWiFS estimated chl-*a* concentrations within the SACCF and MIZ areas for that month. MIZ n is the number of 50×50 km^2 pixels found in the MIZ for each month and is a proxy estimate of the area of the MIZ for each month. The satellite-estimated MIZ is indeterminate for months where sea-ice extent is greater at the end of the month than at the beginning of the month (hence the single point data for some months). Also, chl-*a* values for the MIZ can be relatively high when the area is small and close to shore (March/April).

upper limit for defining this area. For example, the following factors could be enhancing or limiting biomass blooms: (1) strong winds may deepen the MLD, thereby diluting the bloom; and/or driving phytoplankton to depths where light is insufficient to maintain growth; (2) nutrients (either macro or trace) in the area may have been depleted so that significant growth cannot be supported; (3) the sea-ice retreat is anomalously early when light levels are too low to sustain a phytoplankton bloom and/or (4) the *magnitude* of spring sea ice is low, because the overall winter sea-ice extent was low, thus resulting in a spatially less extensive spring bloom. These caveats notwithstanding, we can use the satellite images to compute the potential area of the MIZ and the average chl-*a* concentration within this area for each month (Fig. 7) to create a time series of these two parameters.

The green curves in Fig. 7 show, as in Fig. 4, the chl-*a* concentrations (mg m^{-3}) for the SACCF zone. However, in Fig. 7, the green curves give the average for all three regions (south, middle and north). In contrast with Fig. 4, the red curves in Fig. 7 show the average chl-*a* concentration within our satellite-determined MIZ (i.e., the average chl-*a* concentration in the area defined by the location of sea ice at the beginning and ending of each month). The grey curves (MIZ n) give the number of pixels within this defined area and is proportional to the MIZ area. These data show that early in the season, during October/November when the MIZ area is relatively large and generally seaward of the shelf break, chl-*a* concentration is relatively low. Inspection of individual monthly images (S.M. 1) show that most pigment biomass during this period is confined to the SACCF zone and that any contribution from the MIZ, in spite of its large area during this period, is relatively low. During December, sea ice retreats to over the shelf and the contribution from the MIZ increases. Pigment biomass contribution from the MIZ peaks in January and February but, as noted above, it is not possible from inspection of the monthly images alone to attribute this increase to melt water stability or to other factors influencing production over the shelf.

3.5.2. *Southern Antarctic Circumpolar Current Front*

Figs. 4 and 7 strongly suggest that pigment biomass early in the season is driven by processes associated with the SACCF and that the SACCF may be important in determining the location and seasonal progression of enhanced pigment biomass. Fig. 6B, November 1998, shows a pattern with elevated chl-*a* within the SACCF zone that is fully outside the MIZ as defined here. The zonal averages for the SACCF (green curves in Fig. 4) indicate that this zone, seaward of the shelf break, blooms early in the season but then shows little activity throughout the remainder of the season.

3.5.3. *On-to-offshore differences in the MIZ influence on blooms*

The spring sea-ice retreat in the WAP region is highly variable from year-to-year and from off-to-onshore (Stammerjohn et al., 2008b). For example, during the period under discussion (1997–2004) there were highly anomalous years when sea-ice retreat was early or late across the *entire* extended grid region, but there also were years when the retreat was early offshore but late inshore, and vice-versa. Observations to date suggest that in the offshore region during October and November a late sea-ice retreat (Fig. 6D, November 2002) leads to relatively low pigment biomass and an early retreat (Fig. 6A and C, November 1998, November 2001) to high biomass. Conversely, in the inshore region during December to January a late sea-ice retreat (Fig. 6G, January 2002) leads to high biomass whereas an early retreat (Fig. 6E and H, January 1999, January 2003) leads to relatively low biomass.

4. Discussion

Mechanisms underlying the observed variability in pigment biomass include factors that can control growth rates (temperature, light and nutrients) and/or the accumulation of cells in the euphotic zone and hence population growth (grazing, water-column stability and sinking). Above we carried out a space/time analysis of pigment biomass within an extended grid area of the WAP region, which highlighted both on-to-offshore and alongshore patterns. The data were averaged and analyzed along on-to-offshore biogeochemical provinces (as described in Section 1.2) to assist in distinguishing different underlying mechanisms. In addition, the data were averaged and analyzed along north–south (alongshore) sections to assist in distinguishing possible long-term changes driven by global warming and changing trophic structure driven by climate migration (Smith et al., 2003a, c).

Fig. 4 provide time-series data that correspond to these functional subdivisions. The offshore (Fig. 4, blue curves) POOZ area is north of the pack ice and south of the Polar Front and has been characterized as a HNLC area, where phytoplankton apparently lack the capacity to fully utilize abundant macronutrients (Minas and Minas, 1992). Within the POOZ, chl-*a* values are low (<0.2 mg m^{-3}), and seasonal variability is typically within a factor of two, while interannual variability is low relative to the other regions. It is likely that both the seasonal cycle and low values observed within the POOZ are a baseline for chlorophyll concentrations in the Southern Ocean.

Within our extended grid, the relatively productive CCSZ and SACCF zones are also within the SIZ which is annually swept by

the relatively narrow (50–250 km wide) marginal ice zone (MIZ, that area where sea-ice melt water influences water-column stability). These areas contain the highest pigment biomass concentrations and show strong seasonal and interannual variability that can vary at least 7-fold. During the 7-year period of our analysis, the SACCF zone (roughly the area 200–400 km offshore of the Peninsula) showed the highest peak chl-*a* values during spring blooms (green curves in Fig. 4). It is noteworthy that these SACCF surface waters appear to sustain a spring bloom in every year that sea ice had departed the zone (5 of 7 years). It is likely that mechanisms associated with both the SACCF and sea-ice related melt water stability influenced the observed spring blooms in this zone. In spite of the relatively high spring chl-*a* peaks, the integrated seasonal biomass within the SACCF zone is usually less than that over the shelf (CCSZ).

It remains to be understood why the SACCF zone (that area roughly parallel to and seaward of the shelf break, where the SACCF is likely to have influence) does not maintain higher levels of pigment biomass throughout the season as indicated by the very low values from January/February through April within this frontal zone. We can hypothesize that during winter the surface waters of the SACCF are subjected to deep mixing and renewal of both marco and micro nutrients. Within the extended grid, the SACCF is bounded by the shelf break of the Antarctic Peninsula to the south and east so that the flow regime (geostrophic volume transport of tens of Sv—see Orsi et al., 1995; Turner and Owens, 1995; Pollard et al., 1995; Martinson et al., 2008) associated with this front remains relatively fixed.

Whitehouse et al. (1995) and Boyd et al. (1995) discuss inorganic nutrients and phytoplankton production, respectively, for the waters of this frontal region, which they show sustain a spring bloom (note that the UK "STERNA" study area in the Bellingshausen Sea as part of the Southern Ocean JGOFS program, along 85°W where Whitehouse and Boyd et al. did their work, is just to the west of our extended grid). However, they also show that these surface waters have limited micro-nutrients that are likely to be depleted by a few months of phytoplankton growth. Thus, a plausible hypothesis for the dominant spatial patterns observed in October/November is that SACCF waters give rise to a spring bloom in these months followed by micro-nutrient (iron) depletion in late spring and summer until subsequent deep mixing and nutrient renewal the following winter.

An alternative, or corollary, hypothesis is that as the season progresses the area of elevated biomass associated with the SACCF will be found deeper in the water column and thus not detected by a satellite ocean-color sensor. Korb et al. (2004), reporting on observations to the east of the Peninsula, noted a subsurface chl-*a* max associated with the SACCF that was undetectable in a monthly composite ocean-color image. Garibotti et al. (2003, 2005) found evidence for a deep chl-*a* maximum off the shelf of the WAP area that most likely is not detected by ocean-color satellite sensors. These alternative hypotheses, with respect to phytoplankton biomass associated with the SACCF, need to be tested by means of *in situ* seasonal observations. Interannual variability could, or might also, be associated with variable upwelling of UCDW associated with the SACCF. According to Martinson et al. (2008) there has been an upward trend in heat content on the shelf, suggesting more frequent or more intense upwelling of UCDW over the period of observations presented here (1997–2004). In turn, this could explain the consistent bloom along the SACCF in November observed over this period.

The time series in Fig. 7 show that the MIZ has relatively little influence on pigment biomass early in the season and seaward of the shelf break. This is likely due to relatively low irradiance levels, high winds and deep mixing during late spring early summer. In contrast, Fig. 7 shows that the MIZ contributes to productivity during summer over the shelf but *in situ* data are necessary to fully quantify this contribution. Inspection of monthly images show that the MIZ has relatively high values of pigment biomass (4–5 mg chl-*a* m^{-3}) inside Marguerite Bay; however, these values are not included in the analysis as they lie outside of our grid.

Links between water-column stabilization induced by the spring melt of sea ice and phytoplankton blooms within the retreating MIZ are suggested, but not proven, by these observations. An analysis of the images in S.M. 1 suggest that the spatial patterns observed in satellite-derived chl-*a* and sea-ice extent are consistent with (57%), or at least not in conflict with (an additional 28%), the hypothesis that the MIZ has a major impact on pigment biomass in this region. Regardless of the mechanism, these observations show that the seasonal timing of sea-ice coverage is a critical factor in determining the subsequent space/time development of phytoplankton blooms during the spring as discussed in relation to Figs. 4, 6 and 7. In addition, a spatial cross correlation analysis of January SeaWiFS chl-*a* patterns and ship-determined MLD (not shown) shows strong spatial correlation ($r = 0.707$). This further supports previous findings (Holm-Hansen and Mitchell, 1991; Garibotti et al., 2005) that upper water-column stability, and its influence on solar radiation available to phytoplankton, is a dominant factor in regulating phytoplankton stocks within this region.

Fig. 5 shows that there is a statistically significant relationship between our satellite observations and the Nino3.4 Index (r^2 is 25% between chl-*a* and the Nino3.4 Index). The highest interannual chl-*a* values occurred during strong La Niña events (1998–1999, 1999–2000 and 2000–2001) of which two also coincided with strong positive SAM events (1998–1999 and 1999–2000). Chl-*a* values also were high in 2001–2002, which coincided with a strong positive SAM event (though the Nino3.4 index indicated near neutral ENSO conditions). In contrast, chl-*a* values were low during the two El Nino events that occurred within our observational period: 1997–1998 and 2002–2003.

As mentioned previously, the high-latitude atmospheric response to La Niña and/or positive SAM consists of strong north-westerly winds in the WAP region during spring-to-autumn, whereas during El Nino and/or negative SAM events, weak southerly winds are often present (Fogt and Bromwich, 2006; Stammerjohn et al., 2008a). Strong north-westerly winds during the spring retreat contribute to an early sea-ice retreat offshore of the PAL LTER region. However, inshore the retreat may be delayed if the wind intensity and direction were such that it literally piles sea ice along the coast (i.e., by rafting and thus mechanically thickening the ice cover) as happened quite dramatically in 2001–2002 (Massom et al., 2006) and to a lesser degree in 1999–2000 and 2000–2001. If the winds are more northerly (than north-westerly), then sea ice may be advected southward out of the PAL LTER region, thus contributing to an early sea-ice retreat both offshore and inshore as happened in 1998–1999. Conversely, when winds are weak or southerly as during El Nino and/or—SAM events, the spring retreat is late, particularly offshore. In general, Fig. 5 quite strikingly shows that the high-latitude atmosphere–ice response to ENSO and SAM variability can strongly influence pigment biomass variability, at least as observed over the 1997–2004 period.

The productive CCSZ (Fig. 4, red curves) displays (1) considerable seasonal and interannual variability, (2) often exhibits relatively large blooms, (3) may partially exhaust the supply of macronutrients (Holm-Hansen et al., 1989), (4) can be significantly influenced by glacial meltwater, particularly the nearshore areas (Dierssen et al., 2002) and (5) was believed to have the highest levels of pigment biomass and phytoplankton productivity (El-Sayed, 1968; Holm-Hansen et al., 1977; Priddle et al., 1986;

Jacques, 1989; Smith and Sakshaug, 1990; Smith et al., 1996b; Garibotti et al., 2003, 2005). The CCSZ is the zone that has been most consistently studied. However, with respect to the above fifth point, the present study indicates consistently high biomass in the SACCF zone during spring, thus rivaling the importance of the CCSZ in regional estimates of pigment biomass.

As noted in the introduction, the WAP area is experiencing one of the most rapid warming trends on the planet, giving rise to: warmer surface air temperatures (particularly in fall and winter), a shorter sea-ice season, and an increase in warm/moist maritime influence over cold/dry continental influence. Hypotheses suggest that the ice-dominated ecosystem, balanced on the ice/water temperature threshold, has the potential for strong non-linear response as the system shifts from ice to water (Smith et al., 2003a, b). Further, we hypothesize that the marine ecosystem within the eWAP will experience a displacement as manifest in changing trophic structure driven by the recent rapid warming. Our analysis in terms of north-to-south sectors is motivated by this hypothesis and provides baseline data for comparison with future observations. The time series (Fig. 4) for the north, mid and south onshore areas often show multiple chl-*a* peaks and more sustained blooms throughout the growing season.

Consistent with previous January cruise-based observations, satellite observations show that near-shore stations (within 40–60 km from the islands and peninsula) have 3–10 times higher pigment biomass than stations 180–200 km offshore during January. However, as the satellite time series data show, this on-to-offshore gradient is reversed earlier during the growing season (October/November) when pigment values seaward of the shelf break are typically higher than over the shelf and near shore. However, as mentioned previously, the high chl-*a* levels that were observed within the SACCF region may be related to an increase in upwelling of upper CDW along the shelf break (and thus the delivery of micro-nutrients) as reported by Martinson et al. (2008) during this same time period (1997–2004). It has been hypothesized that the increased upwelling may be a response to the intensification of the regional atmospheric circulation in conjunction with the strong climate change that is occurring in the AP region. Also, January data from the early 1990s show higher pigment biomass in the northern region (600 line) of the PAL grid (Smith et al., 2001), whereas more recently higher pigment biomass is found in the southern region (200 line) of the PAL grid (Fig. 4). These observations are consistent with the PAL hypothesis that the warming trend along the Antarctic Peninsula will lead to ecosystem migration as the location of mean sea-ice conditions moves poleward with climate warming. The role that the SACCF-related spring bloom may play in modulating ecosystem change is as yet unknown. Data discussed herein do not cover a long enough time period to establish overall trends, however on-going research will continue to address this hypothesis as more data become available.

5. Summary

The SeaWiFS imagery presented here provides the most complete synoptic space/time views of phytoplankton biomass within this region to date. These data provide a seven-year quantification of space/time variability in pigment biomass that geographically extends the Palmer LTER surface observations. Key findings include:

(1) The dominant spatial patterns and seasonal variability of pigment biomass over an extended grid west of the Antarctic Peninsula have been identified. Seasonal climatologies (September through April) and their respective anomalies have been computed. In addition, EOF analysis of the monthly SeaWiFS climatologies show that the first two modes explain more than one-half of the total monthly variability in pigment biomass and that the first mode displays the dominant space/time features of the seasonal and interannual variability. These patterns show that the earliest spring blooms (October/November) begin offshore in the SACCF zone and then are followed by blooms within the MIZ and over the shelf as the season progresses.

(2) Our satellite-based observations provide additional evidence of the influence of the high-latitude atmosphere–ice response to ENSO and SAM variability on pigment biomass variability. Importantly, the satellite-based observations show this influence to be present throughout the extended grid area (Fig. 5). Mechanisms involve an atmosphere–ice response that contributes either to an early spring sea-ice retreat and high biomass offshore (e.g., in response to La Niña and/or positive SAM events) or a late spring sea-ice retreat and low biomass offshore (e.g., in response to El Nino and/or negative SAM events). Inshore, atmosphere–ice interactions with respect to the timing of the coastal sea-ice retreat are more variable (e.g., see next paragraph) and sensitive to wind direction.

(3) There appears to be an on- versus offshore dichotomy with respect to the relationship between sea-ice retreat and subsequent phytoplankton biomass. In general, an early sea-ice retreat offshore followed by a late sea-ice retreat inshore is conducive to high biomass spatially integrated throughout the season (and vice-versa for late sea-ice retreat offshore followed by an early retreat inshore). The role of the MIZ in this dichotomy is another area of active research.

(4) The observations presented here are consistent with several hypotheses related to the growth and decay of phytoplankton blooms within these Antarctic waters. In particular, regional-scale phytoplankton abundance and distribution within the extended grid depends on: (a) nutrient dynamics, variability in UCDW upwelling, and seasonal succession within surface waters of the SACCF zone; (b) dynamics related to sea ice melt within the MIZ for waters over the shelf during the period of late spring early summer; and (c) dynamics related to coastal waters, including possible stabilization by glacial melt water and the influence of CDW over the shelf from late summer to fall. Marguerite Bay shows consistently high levels of pigment biomass during late summer and early fall, underlying the importance of understanding the linkage between the above dynamics and processes influencing production within Marguerite Bay.

(5) The SACCF is a previously unquantified source of primary productivity seaward of the WAP shelf break. Our observations suggest that the SACCF may have a more profound influence on the WAP ecosystem than previously thought. We find relatively high pigment biomass in the SACCF zone during most springs (October/November). The role of this phytoplankton biomass within the WAP ecosystem has yet to be fully elucidated. Further, the role of iron (or other micro-nutrients), the identification of the proximal physio-chemical factors involved in biological enhancement in the SACCF zone and the seasonal variability observed within the SACCF zone require further investigation and point to the need for continuous *in situ* (e.g., mooring, gliders) observations in this region.

Acknowledgments

This research was supported by NSF Grant OPP90-11927 and NASA Grant NAGW 290-3 to R.C. Smith and, most recently, by OPP-0217282 to VIMS (H.Ducklow, PI). Karen Baker provided

data management and Maria Vernet helpful comments on the manuscript.

References

Beardsley, R.C., Limeburner, R., Owens, W.B., 2004. Drifter measurements of surface currents near Marguerite Bay on the western Antarctic Peninsula shelf during Austral summer and fall, 2001 and 2002. Deep-Sea Research II 51 (17–19), 1947–1964.

Behrenfeld, M.J., Boss, E., Siegel, D.A., Shea, D.M., 2005. Carbon-based ocean productivity and phytoplankton physiology from space. Global Biogeochemical Cycles 19 (1), GB1006.

Boyd, P.W., Robinson, C., Savidge, G., Williams, P.J.leB., 1995. Water column and sea-ice primary production during Austral spring in the Bellingshausen Sea. Deep-Sea Research II 42 (4–5), 1177–1200.

Boye, M., van den Berg, C.M.G., de Jong, J.T.M., Leach, H., Croot, P., de Baar, H.J.W., 2001. Organic complexation of iron in the Southern Ocean. Deep-Sea Research I 48 (6), 1477–1497.

Busalacchi, A.J., 2004. The role of the Southern Ocean in global processes: an earth system science approach. Antarctic Science 16, 363–368.

Cane, M.A., Zebiak, S.E., Dolan, S.C., 1986. Experimental forecasts of El Nino. Nature 321 (6073), 827–832.

Carleton, A.M., 2003. Atmospheric teleconnections involving the Southern Ocean. Journal of Geophysical Research 108 (C4), 8080.

Carvalho, L.M.V., Jones, C., Ambrizzi, T., 2005. Opposite phases of the Antarctic Oscillation and relationships with intraseasonal to interannual activity in the Tropics during Austral summer. Journal of Climate 18, 702–718.

Church, J.A., 2001. Climate change: how fast are sea levels rising? Science 294 (5543), 802–808.

Coale, K.H., Johnson, K.S., Chavez, F.P., Buesseler, K.O., Barber, R.T., Brzezinski, M.A., Cochlan, W.P., Millero, F.J., Falkowski, P.G., Bauer, J.E., Wanninkhof, R.H., Kudela, R.M., Altabet, M.A., Hales, B.E., Takahashi, T., Landry, M.R., Bidigare, R.R., Wang, X., Chase, Z., Strutton, P.G., Friederich, G.E., Gorbunov, M.Y., Lance, V.P., Hilting, A.K., Hiscock, M.R., Demarest, M., Hiscock, W.T., Sullivan, K.F., Tanner, S.J., Gordon, R.M., Hunter, C.N., Elrod, V.A., Fitzwater, S.E., Jones, J.L., Tozzi, S., Koblizek, M., Roberts, A.E., Herndon, J., Brewster, J., Ladizinsky, N., Smith, G., Cooper, D., Timothy, D., Brown, S.L., Selph, K.E., Sheridan, C.C., Twining, B.S., Johnson, Z.I., 2004. Southern ocean iron enrichment experiment: carbon cycling in high- and low-Si waters. Science 304 (5669), 408–414.

Comiso, J.C., 1995. Sea-ice geophysical parameters from SSMR and SSM/I data. In: Ideda, M., Dobson, F. (Eds.), Oceanographic Applications of Remote Sensing. CRC Press, Inc., pp. 321–338.

Comiso, J., 2003. Sea ice concentrations derived from the Bootstrap algorithm. In: Maslanik, J., Stroeve, J. (Eds.), DMSP SSM/I Daily Polar Gridded Sea Ice Concentrations. National Snow and Ice Data Center, Digital Media, Boulder, CO.

Comiso, J.C., Cavalieri, D., Parkinson, C., Gloersen, P., 1997. Passive microwave algorithms for sea ice concentration—a comparison of two techniques. Remote Sensing of the Environment 60 (3), 357–384.

Croot, P.L., Andersson, K., Öztürk, M., Turner, D.R., 2004. The distribution and speciation of iron along 6°E in the Southern Ocean. Deep-Sea Research II 51 (22–24), 2857–2879.

Dierssen, H.M., Smith, R.C., 2000. Bio-optical properties and remote sensing ocean color algorithms for Antarctic Peninsula waters. Journal of Geophysical Research 105 (C11), 26,301–26,312.

Dierssen, H.M., Vernet, M., Smith, R.C., 2000. Optimizing models for remotely estimating primary production in Antarctic coastal waters. Antarctic Science 12 (1), 20–32.

Dierssen, H.M., Smith, R.C., Vernet, M., 2002. Glacial meltwater dynamics in coastal waters west of the Antarctic Peninsula. Proceedings of the National Academy of Science 99 (4), 33–45.

Dinniman, M.S., Klinck, J.M., 2004. A model study of circulation and cross-shelf exchange on the west Antarctic Peninsula continental shelf. Deep-Sea Research II 51 (17–19), 2003–2022.

Domack, E., Leventer, A., Burnett, A., Bindschadler, R., Convey, P., Kirby, M. (Eds.), 2003. Antarctic Peninsula Climate Variability: Historical and Paleoenvironmental Perspective, 79. American Geophysical Union, Washington, DC.

Ducklow, H.W., Baker, K., Martinson, D.G., Quetin, L.B., Ross, R.M., Smith, R.C., Stammerjohn, S.E., Vernet, M., Fraser, W., 2007. Marine pelagic ecosystems: the West Antarctic Peninsula. Philosophical Transactions of the Royal Society B 362, 67–94.

El-Sayed, S.Z., 1968. On the productivity of the southwest Atlantic Ocean and the waters west of the Antarctic Peninsula. In: Llano, G.A., Schmitt, W.L. (Eds.), Biology of the Antarctic Seas III. American Geophysical Union, Washington, DC, pp. 15–47.

Fogt, R.L., Bromwich, D.H., 2006. Decadal variability of the ENSO teleconnection to the high latitude South Pacific governed by coupling with the Southern Annular Mode. Journal of Climate 19, 979–997.

Garibotti, I.A., Vernet, M., Ferrario, M.E., Smith, R.C., Ross, R.M., Quetin, L.B., 2003. Phytoplankton spatial distribution in the Western Antarctic Peninsula (Southern Ocean). Marine Ecology Progress Series 261, 21–39.

Garibotti, I.A., Vernet, M., Smith, R.C., Ferrario, M.E., 2005. Interannual variability in the distribution of the phytoplankton standing stock across the seasonal sea-ice zone west of the Antarctic Peninsula. Journal of Plankton Research 27 (8), 825–843.

Gille, S.T., 2002. Warming of the Southern Ocean since the 1950s. Science 295, 1275–1277.

Gordon, H.R., Morel, A.Y., 1983. Remote Assessment of Ocean Color for Interpretation of Satellite Visible Imagery, A Review, Lect. Notes on Coastal and Estuarine Stud., vol. 4. Springer, New York, 114pp.

Gordon, H.R., Clark, D.K., Brown, J.W., Brown, O.B., Evans, R.H., Broenkow, W.W., 1983. Phytoplankton pigment concentrations in the Middle Atlantic Bight: comparison of ship determinations and Coastal Zone Color Scanner measurements. Applied Optics 22, 20–36.

Hall, A., Visbeck, M., 2002. Synchronous variability in the Southern Hemisphere atmosphere, sea ice, and ocean resulting from the annular mode. Journal of Climate 15 (21), 3043–3057.

Harangozo, S.A., 2000. A search for ENSO teleconnections in the west Antarctic Peninsula climate in Austral winter. International Journal of Climatology 20 (6), 663–679.

Harangozo, S.A., 2006. Atmospheric circulation impacts on winter maximum sea ice extent in the west Antarctic Peninsula region (1979–2001). Geophysical Research Letters 33, 〈doi:10.1029/2005GL024978〉.

Harris, C., Stonehouse, B. (Eds.), 1991. Antarctica and Global Climatic Change. Belhaven Press, London, 198pp.

Hart, T.J., 1942. Phytoplankton periodicity in Antarctic surface waters. Discovery Reports 21, 261–356.

Hofmann, E.E., Klinck, J.M., 1998. Thermohaline variability of the waters overlying the West Antarctic Peninsula Continental Shelf. In: Jacobs, S.S., Weiss, R.F. (Eds.), Ocean, Ice, and Atmosphere: Interactions. Antarctic Research Series, vol. 75. American Geophysical Union, Washington, DC, pp. 67–81.

Hofmann, E.E., Klinck, J.M., Lascara, C.M., Smith, D., 1996. Water mass distribution and circulation West of the Antarctic Peninsula and including Bransfield Strait. In: Ross, R.M., Hofmann, E.E., Quetin, L.B. (Eds.), Foundations for Ecological Research West of the Antarctic Peninsula. Antarctic Research Series. American Geophysical Union, Washington, DC, pp. 61–80.

Holm-Hansen, O., Mitchell, B.G., 1991. Spatial and temporal distribution of phytoplankton and primary production in the western Bransfield Strait region. Deep-Sea Research 38 (8–9), 961–980.

Holm-Hansen, O., El-Sayed, S.Z., Franceschini, G.A., Cuhel, R.L., 1977. Primary production and the factors controlling phytoplankton growth in the Southern Ocean. In: Llano, G.A. (Ed.), Adaptations Within Antarctic Ecosystems: Proceedings of the Third SCAR Symposium on Antarctic Biology. Sponsored by the Scientific Committee for Antarctic Research (SCAR) and the International Union of Biological Sciences and held under the Auspices of the United States National Academy of Sciences. Washington, DC, August 26–30, 1974. Gulf Publishing Co., Houston, pp. 11–50.

Holm-Hansen, O., Mitchell, B.G., Hewes, C.D., Karl, D.M., 1989. Phytoplankton blooms in the vicinity of Palmer Station, Antarctica. Polar Biology 10, 49–57.

Hovis, W.A., Clark, D.K., Anderson, F., et al., 1980. Nimbus-7 Coastal Zone Color Scanner: system description and initial imagery. Science 210 (4465), 60–63.

Jacobs, S.S., Comiso, J.C., 1997. Climate variability in the Amundsen and Bellingshausen Seas. Journal of Climate 10, 697–709.

Jacques, G., 1989. Primary production in the open Antarctic Ocean during Austral summer. A review. Vie et Milieu 39, 1–17.

Kalnay, E., Kanamitsu, M., Kistler, R., Collins, W., Deaven, D., Gandin, L., Iredell, M., Saha, S., White, G., Woollen, J., Zhu, Y., Chelliah, M., Ebisuzaki, W., Higgins, W., Janowiak, J., Mo, K.C., Ropelewski, C., Wang, J., Leetmaa, A., Reynolds, R., Jenne, R., Joseph, D., 1996. The NCEP/NCAR 40-year reanalysis project. Bulletin of the American Meteorological Society 77, 437–471.

Kellogg, W.W., 1983. Feedback mechanisms in the climate system affecting future levels of carbon dioxide. Journal of Geophysical Research (C Ocean Atmosphere) Special issue: Bern Co sub (2) symposium 88 (2), C2,1263–C2,1269.

Kennedy, C., 2002. POTUS and the fish. Science 297, 477.

King, J.C., 1994. Recent climate variability in the vicinity of the Antarctic Peninsula. International Journal of Climatology 14 (4), 357–369.

King, J.C., Harangozo, S.A., 1998. Climate change in the western Antarctic Peninsula since 1945: observations and possible causes. Annals of Glaciology 27, 571–575.

King, J.C., Turner, J., Marshall, G.J., Connolley, W.M., Lachlan-Cope, T.A., 2003. Antarctic Peninsula climate variability and its causes as revealed by instrumental records. In: Domack, E., Burnett, A., Convey, P., Kirby, M., Bindschadler, R. (Eds.), Antarctic Peninsula Climate Variability: a historical and Paleoenvironmental Perspective. Antarctic Research Series, vol. 79. American Geophysical Union, Washington, DC, pp. 17–30.

Klinck, J.M., 1998. Heat and salt changes on the continental shelf west of the Antarctic Peninsula between January 93 and January 94. Journal of Geophysical Research 103 (C4), 7617–7636.

Korb, R.E., Whitehouse, M.J., Ward, P., 2004. SeaWiFS in the southern ocean: spatial and temporal variability in phytoplankton biomass around South Georgia. Deep-Sea Research II 51 (1–3), 99–116.

Kwok, R., Comiso, J.C., 2002. Southern Ocean climate and sea ice anomalies associated with the Southern Oscillation. Journal of Climate 15 (5), 487–501.

Lefebvre, W., Goosse, H., Timmermann, R., Fichefet, T., 2004. Influence of the Southern Annular Mode on the sea ice-ocean system. Journal of Geophysical Research 109, C09005.

L'Heureux, M.L., Thompson, D.W.J., 2006. Observed relationships between the El Nino-Southern Oscillation and the extratropical zonal-mean circulation. Journal of Climate 19, 276–287.

Liu, J., Yuan, X., Rind, D., Martinson, D.G., 2002a. Mechanism study of the ENSO and southern high latitudes climate teleconnections. Geophysical Research Letters 29 (14).
Liu, J., Martinson, D.G., Yuan, X., Rind, D., 2002b. Evaluating Antarctic sea ice variability and its teleconnections in global climate models. International Journal of Climatology 22 (8), 885–900.
Liu, J., Schmidt, G.A., Martinson, D.G., Rind, D., Russell, G., Yuan, X., 2003. Sensitivity to sea ice to physical parameterizations in the GISS global climate model. Journal of Geophysical Research: Oceans 108 (C2).
Liu, J., Curry, J.A., Martinson, D.G., 2004. Interpretation of recent Antarctic sea ice variability. Geophysical Research Letters 31, L02205.
Longhurst, A., 1998. Ecological Geography of the Sea. Academic Press, San Diego, 398pp.
Marshal, G.J., 2003. Trends in the Southern Annular Mode from observations and reanalyses. Journal of Climate 16, 4134–4143.
Marshall, G.J., Stott, P.A., Turner, J., Connolley, W.M., King, J.C., Lachlan-Cope, T.A., 2004. Causes of exceptional atmospheric circulation changes in the Southern Hemisphere. Geophysical Research Letters 31 (L14205).
Martin, J.H., Fitzwater, S.E., 1988. Iron deficiency limits phytoplankton growth in the north-east Pacific subarctic. Nature 331, 341–343.
Martin, J.H., Gordon, R.M., Fitzwater, S.E., 1990. Iron in Antarctic waters. Nature 345, 156–158.
Martinson, D.G., Iannuzzi, R.A., 2003. Spatial/temporal patterns in Weddell gyre characteristics and their relationship to global climate. Journal of Geophysical Research 108 (C4).
Martinson, D.G., Stammerjohn, S.E., Iannuzzi, R.A., Smith, R.C., Vernet, M., 2008. Palmer, Antarctica, long-term ecological research program first 12 years: physical oceanography, spatio-temporal variability. Deep-Sea Research II, this issue [doi:10.1016/j.dsr2.2008.04.038].
Massom, R.A., Stammerjohn, S.E., Smith, R.C., Pook, M.J., Iannuzzi, R.A., Adams, N., Martinson, D.G., Vernet, M., Fraser, W.R., Quetin, L.B., Ross, R.M., Massom, Y., Krouse, H.R., 2006. Extreme anomalous atmospheric circulation in the west Antarctic Peninsula Region in Austral spring and summer 2001/02, and its profound impact on sea ice and biota. Journal of Climate 19, 3544–3571.
McCarthy, J.J., Canziani, O.F., Leary, N.A., Dokken, D.J., White, K.S. (Eds.), 2001. Climate Change 2001, Impacts, Adaptation, and Vulnerability, Intergovernmental Pannel on Climate Change, Cambridge University Press, 1032pp.
Measures, C.I., Vink, S., 2001. Dissolved Fe in the upper waters of the Pacific sector of the Southern Ocean. Deep-Sea Research II 48 (19–20), 3913–3941.
Minas, H.J., Minas, M., 1992. Net community production in "high nutrient-low chlorophyll" waters of the tropical and Antarctic Oceans. Oceanologica Acta 15, 145–162.
Mitchell, B.G., Holm-Hansen, O., 1991. Bio-optical properties of Antarctic Peninsula waters: differentiation from temperate ocean models. Deep-Sea Research 38 (8/9), 1009–1028.
Moffit, C., Beardsley, R., Owens, B., van Lipzig, N., 2008. A first description of the Antarctic Peninsula Coastal Current. Deep-Sea Research II 55 (3–4), 277–293.
Moline, M.A., Prezelin, B.B., 1996. Long-term monitoring and analyses of physical factors regulating variability in coastal Antarctic phytoplankton biomass, in situ productivity and taxonomic composition over subseasonal, seasonal and interannual time scales. Marine Ecology Progress Series 145, 143–160.
Moore, J.K., Abbott, M.R., 2000. Phytoplankton chlorophyll distributions and primary production in the Southern Ocean. Journal of Geophysical Research 105 (C12), 28,709–28,722.
Moore, J.K., Abbott, M.R., Richman, J.G., Smith, W.O., Cowles, T.J., Coale, K.H., Gardner, W.D., Barber, R.T., 1999. SeaWiFS satellite ocean color data from the Southern Ocean. Geophysical Research Letters 26 (10), 1465–1468.
Nelson, D.M., Smith, W.O., Gordon, L.I., Huber, B.A., 1987. Spring distributions of density, nutrients, and phytoplankton biomass in the ice edge zone of the Weddell-Scotia Sea. Journal of Geophysical Research 92, 7,181–7,190.
O'Reilly, J.E., Maritorena, S., Mitchell, B.G., Siegel, D.A., Carder, K.L., Garver, S.A., Kahru, M., McClain, C., 1998. Ocean color chlorophyll algorithms for SeaWiFS. Journal of Geophysical Research 103 (C11), 24937–24953.
O'Reilly, J.E., Maritorena, S., O'Biren, M.C., Siegel, D.A., Toole, D.A., Menzies, D.W., Smith, R.C., Mueller, J.L., Mitchell, B.G., Kahru, M., Chavez, F.P., Strutten, P., Cota, G.F., Hooker, S.B., McClain, C.R., Carder, K.L., Muller-Karger, F., Harding, L., Magnuson, A., Phinney, D., Moore, G.F., Aiken, J., Arrigo, K.R., Letelier, R.M., Culver, M., 2000. SeaWiFS postlaunch calibration and validation analyses, part 3. In: Hooker, S.B., Firestone, E.R. (Eds.), SeaWiFS Postlaunch Technical Report Series, NASA/TM-2000-206892, vol. 11. NASA/GSFC, Greenbelt, MD, p. 49.
Orsi, A.H., Whitworth, T., Nowlin, W.D., 1995. On the meridional extent and fronts of the Antarctic Circumpolar Current. Deep-Sea Research I 42 (5), 641–673.
Parkinson, C.L., 2002. Trends in the length of the Southern Ocean sea ice season, 1979–1999. Annals of Glaciology 34, 435–440.
Parkinson, C.L., 2004. Southern Ocean sea ice and its wider linkages: insights revealed from models and observations. Antarctic Science 16 (4), 387–400.
Pollard, R.T., Read, J.F., Allen, J.T., Griffiths, G., Morrison, A.I., 1995. On the physical structure of a front in the Bellingshausen Sea. Deep-Sea Research 42 (4–5), 955–982.
Priddle, J.J., Hawes, I., Ellis-Evans, J.C., 1986. Antarctic aquatic ecosystems as habitats for phytoplankton. Biology Review 61, 199–238.
Rind, D., Healy, R., Parkinson, C., Martinson, D., 1995. The role of sea ice in $2 \times CO_2$ climate model sensitivity. Part I: the total influence of sea ice thickness and extent. Journal of Climate 8 (3), 449–463.
Rind, D., Chandler, M., Lerner, J., Martinson, D.G., Yuan, X., 2001. Climate response to basin-specific changes in latitudinal temperature gradients and implications for sea ice variability. Journal of Geophysical Research 106 (D17), 20161–20173.
Ross, R.M., Hofmann, E.E., Quetin, L.B. (Eds.), 1996. Foundations for Ecological Research West of the Antarctic Peninsula. Antarctic Research Series 70, vol. 70. American Geophysical Union, Washington, DC, 448pp.
Rue, E.L., Bruland, K.W., 1995. Complexation of iron(III) by natural organic ligands in the Central North Pacific as determined by a new competitive ligand equilibration/adsorptive cathodic stripping voltammetric method. Marine Chemistry 50 (1–4), 117–138.
Sarmiento, J.L., Le Quere, C., 1996. Oceanic carbon dioxide uptake in a model of century-scale global warming. Science 274 (5291), 1346–1350.
Sarmiento, J.L., Hughes, T.M.C., Stougger, R.J., Manabe, S., 1998. Simulated response of the ocean carbon cycle to anthropogenic climate warming. Nature 393, 245–249.
Siegel, D.A., Thomas, A.C., Marra, J., 2004. Views of ocean processes from the sea-viewing wide field-of-view sensor mission: introduction to the first special issue. Deep-Sea Research II 51 (1–3), 1–3.
Silvestri, G.E., Vera, C.S., 2003, Antarctic oscillation signal on precipitation anomalies over southeastern South America. Geophysical Research Letters 30, ⟨doi:10.1029/2003GL018277⟩.
Simmonds, I., 2003. Modes of atmospheric variability over the Southern Ocean. Journal of Geophysical Research 108 (C4).
Simmonds, I., Jacka, T.H., 1995. Relationships between the interannual variability of Antarctic sea ice and the Southern Oscillation. Journal of Climate 8, 637–647.
Simmonds, I., King, J.C., 2004. Global and hemispheric climate variations affecting the Southern Ocean. Antarctic Science 16 (4), 401–413.
Smetacek, V., De Baar, H.J.W., Bathmann, U.V., Lochte, K., Van Der Loeff, M.M.R., 1997. Ecology and biogeochemistry of the Antarctic Circumpolar Current during Austral spring: a summary of southern ocean JGOFS cruise ANT X/6 of R.V. *Polarstern*. Deep-Sea Research II 44 (1–2), 1–21.
Smith, W.O., Nelson, D.M., 1985. Phytoplankton bloom produced by a receding ice edge in the Ross Sea: spatial coherence with the density field. Science 227, 163–166.
Smith, W.O., Nelson, D.M., 1986. Importance of ice edge phytoplankton production in the Southern Ocean. Bioscience 36, 51–257.
Smith, W.O., Sakshaug, E., 1990. Polar phytoplankton. In: Smith, W.O. (Ed.), Polar Oceanography. Academic Press, San Diego, pp. 477–525.
Smith, R.C., Stammerjohn, S.E., 2001. Variations of surface air temperature and sea ice extent in the western Antarctic Peninsula (WAP) region. Annals of Glaciology 33, 493–500.
Smith, R.C., Baker, K.S., Fraser, W.R., Hofmann, E.E., Karl, D.M., Klinck, J.M., Quetin, L.B., Prezelin, B.B., Ross, R.M., Trivelpiece, W.Z., Vernet, M., 1995. The Palmer LTER: a long-term ecological research program at Palmer Station, Antarctica. Oceanography 8 (3), 77–86.
Smith, R.C., Stammerjohn, S.E., Baker, K.S., 1996a. Surface air temperature variations in the western Antarctic peninsula region. In: Ross, R.M., Hofmann, E.E., Quetin, L.B. (Eds.), Foundations for Ecological Research West of the Antarctic Peninsula. Antarctic Research Series 70. American Geophysical Union, Washington, DC, pp. 105–121.
Smith, R.C., Dierssen, H.M., Vernet, M., 1996b. Phytoplankton biomass and productivity in the western Antarctic peninsula region. In: Ross, R.M., Hofmann, E.E., Quetin, L.B. (Eds.), Foundations for Ecological Research West of the Antarctic Peninsula. AGU Antarctic Research Series. American Geophysical Union, Washington, DC, pp. 333–356.
Smith, R.C., Baker, K.S., Byers, M.L., Stammerjohn, S.E., 1998a. Primary productivity of the palmer long term ecological research area and the Southern Ocean. Journal of Marine Systems 17 (1–4), 245–259.
Smith, R.C., Baker, K.S., Stammerjohn, S.E., 1998b. Exploring sea ice indexes for polar ecosystem studies. BioScience 48 (2), 83–93.
Smith, D.A., Hofmann, E.E., Lascara, C.M., Klinck, J.M., 1999a. Hydrography and circulation of the west Antarctic Peninsula continental shelf. Deep-Sea Research I 46 (6), 925–949.
Smith, R.C., Ainley, D., Baker, K., Domack, E., Emslie, S., Fraser, W., Kennett, J., Leventer, A., Mosley-Thompson, E., Stammerjohn, S., Vernet, M., 1999b. Marine ecosystem sensitivity to climate change. BioScience 49 (5), 393–404.
Smith, R.C., Baker, K.S., Dierssen, H.M., Stammerjohn, S.E., Vernet, M., 2001. Variability of primary production in an Antarctic marine ecosystem as estimated using a multi-scale sampling strategy. American Zoologist 41, 40–56.
Smith, R.C., Fraser, W.R., Stammerjohn, S.E., 2003a. Climate variability and ecological response of the marine ecosystem in the western Antarctic Peninsula (WAP) region. In: Greenland, D., Goodin, D., Smith, R.C. (Eds.), Climate Variability and Ecosystem Response at Long-Term Ecological Research (LTER) Sites. Oxford Press, New York.
Smith, R.C., Fraser, W.R., Stammerjohn, S.E., Vernet, M., 2003b. Palmer long-term ecological research on the Antarctic marine ecosystem. In: Domack, E.W., Leventer, A., Burnett, A., Convey, P., Kirby, M., Bindschadler, R. (Eds.), Antarctic Peninsula Climate Variability: a Historical and Paleoenvironmental Perspective. American Geophysical Union, Washington, DC, pp. 131–144.
Smith, R.C., Yuan, X., Liu, J., Martinson, D.G., Stammerjohn, S.E., 2003c. The quasi-quintennial time scale-synthesis. In: Greenland, D., Goodin, D., Smith, R.C. (Eds.), Climate Variability and Ecosystem Response at Long-Term Ecological Research (LTER) Sites. Oxford Press, New York, pp. 196–206.

Stammerjohn, S.E., 1993. Spatial and temporal variability in southern ocean sea ice coverage. M.A. Thesis, University of California Santa Barbara, Santa Barbara, 117pp.

Stammerjohn, S.E., Smith, R.C., 1996. Spatial and temporal variability of western Antarctic Peninsula sea ice coverage. In: Ross, R.M., Hofmann, E.E., Quetin, L.B. (Eds.), Foundations for Ecological Research West of the Antarctic Peninsula. Antarctic Research Series. American Geophysical Union, Washington, DC, pp. 81–104.

Stammerjohn, S.E., Smith, R.C., 1997. Opposing Southern Ocean climate patterns as revealed by trends in regional sea ice coverage. Climatic Change 37 (4), 617–639.

Stammerjohn, S.E., Drinkwater, M.R., Smith, R.C., Liu, X., 2003. Ice–atmosphere interactions during sea-ice advance and retreat in the western Antarctic Peninsula region. Journal of Geophysical Research 108 (C10).

Stammerjohn, S.E., Martinson, D.G., Smith, R.C., Yuan, X., Rind, D. 2008a. Trends in Antarctic sea ice retreat and advance and their relation to El Nino-Southern Oscillation and Southern Annular Mode variability. Journal of Geophysical Research, 113, C03S90, doi:10.1029/2007JC004269.

Stammerjohn, S.E., Martinson, D.G., Smith, R.C., Iannuzzi, R.A., 2008b. Sea ice in the Western Antarctic Peninsula region: spatio-temporal variability from ecological and climate change perspectives. Deep-Sea Research II, this issue [doi:10.1016/j.dsr2.2008.04.026].

Stark, P., 1994. Climatic warming in the central Antarctic Peninsula area. Weather 49 (6), 215–220.

Sullivan, C., Arrigo, K., McClain, C., Comiso, J., Firestone, J., 1993. Distributions of phytoplankton blooms in the Southern Ocean. Science 262, 1832–1837.

Thompson, D.W., Solomon, S., 2002. Interpretation of recent Southern Hemisphere climate change. Science 296, 895–899.

Thompson, D.W., Wallace, J.M., 2000. Annual modes in the extratropical circulaton. Part I: month-to-month variability. Journal of Climate 13, 1000–1016.

Tréguer, P., Jacques, G., 1992. Dynamics of nutrient and phytoplankton and cycles of carbon, nitrogen and silicon in the Southern Ocean: a review. Polar Biology 12, 149–162.

Turner, D.R., Owens, N.J.P., 1995. A biogeochemical study in the Bellingshausen Sea: overview of the STERNA 1992 expedition. Deep-Sea Research II 42 (4–5), 907–932.

Turner, J., Colwell, S.R., Harangozo, S., 1997. Variability of precipitation over the coastal western Antarctic Peninsula from synoptic observations. Journal of Geophysical Research 102 (D12), 13999–14007.

Turner, J., Lachlan-Cope, T., Cowell, S., Marshall, G.J., 2005. A positive trend in western Antarctic Peninsula precipitation over the last 50 years reflecting regional and Antarctic-wide atmospheric circulation changes. Annals of Glaciology 41, 85–91.

Tynan, C.T., 1998. Ecological importance of the southern boundary of the Antarctic circumpolar current. Nature 392, 708–710.

Vaughan, D.G., Marshall, G.J., Connolley, W.M., King, J.C., Mulvaney, R., 2001. Devil in the detail. Science 293 (5536), 1777–1779.

Vaughan, D.G., Marshall, G.J., Connolley, W.M., Parkinson, C., Mulvaney, R., Hodgson, D.A., King, J.C., Pudsey, C.J., Turner, J., 2003. Recent rapid regional climate warming on the Antarctic Peninsula. Climatic Change 60 (3), 243–274.

Venegas, S.A., Drinkwater, M.R., Schaffer, G., 2001. Coupled oscillations in Antarctic sea-ice and atmosphere in the South pacific sector. Geophysical Research Letters 28 (17), 3301–3304.

Walsh, J.E., 1983. The role of sea ice in climatic variability: theories and evidence. Atmosphere-Ocean 21 (3), 229–242.

Waters, K.J., Smith, R.C., 1992. Palmer LTER: a sampling grid for the Palmer LTER program. Antarctic Journal of the United States 27 (5), 236–239.

Watkins, A.B., Simmonds, I., 2000. Current trends in Antarctic sea ice: the 1990s impact on a short climatology. Journal of Climate 13 (24), 4441–4451.

White, W.B., Peterson, R.G., 1996. An Antarctic circummpolar wave in surface pressure, wind, temperature and sea-ice extent. Nature 380 (6576), 699–702.

Whitehouse, M.J., Priddle, J., Woodward, E.M.S., 1995. Spatial variability of inorganic nutrients in the marginal ice zone of the Bellingshausen Sea during the Austral spring. Deep-Sea Research II 42 (4–5), 1047–1058.

Yuan, X., 2004. ENSO-related impacts on Antarctic sea ice: a synthesis of phenomenon and mechanisms. Antarctic Science 16 (4), 415–425.

Yuan, X., Martinson, D.G., 2000. Antarctic sea ice extent variability and its global connectivity. Journal of Climate 13 (10), 1697–1717.

Yuan, X., Martinson, D.G., 2001. The Antarctic dipole and its predictability. Geophysical Research Letters 28 (18), 3609–3612.

Zwally, H.J., Comiso, J.C., Parkinson, C.L., Cavalieri, D.J., Gloersen, P., 2002. Variability of Antarctic sea ice 1979–1998. Journal Geophysical Research, Oceans 107 (C5).